# Using Copernicus Sentinel-2 and Sentinel-3 data to monitor harmful algal blooms in Southern Chile during the COVID-19 lockdown

Cristina V. Rodríguez-Benito[a], Gabriel Navarro[b], Isabel Caballero[b],*

[a] *Mariscope Ingeniería, Puerto Montt, Chile*
[b] *Instituto de Ciencias Marinas de Andalucía (ICMAN), Consejo Superior de Investigaciones Científicas (CSIC), Puerto Real 11510, Cádiz, Spain*

ABSTRACT

During the southern summer of 2020, large phytoplankton blooms were detected using satellite technology in Chile (western Patagonia), where intensive salmonid aquaculture is carried out. Some harvesting sites recorded massive fish mortalities, which were associated with the presence of the dinoflagellate species *Cochlodinium* sp. The bloom included other phytoplankton species, as *Lepidodinium chlorophorum*, which persistently changed the colour of the ocean to green. These blooms coincided with the government-managed emergency lockdown due to the COVID-19 pandemic. Local in situ sampling was slowed down. However, imagery from the Copernicus programme allowed operational monitoring. This study shows the benefits of both Sentinel-3 and Sentinel-2 satellites in terms of their spectral, spatial and temporal capabilities for improved algal bloom monitoring. These novel tools, which can foster optimal decision-making, are available for delivering early alerts in situations of natural catastrophes and blockages, such as those occurred during the global COVID-19 lockdown.

## 1. Introduction

Proliferations of phytoplankton blooms are common events in coastal environments. Some phytoplankton blooms are perceived as harmful, if the species presented causes massive fish kills, contaminate seafood with toxins and alter the ecosystems (Cullen, 2008). For microalgae producers of potent biotoxins, harmful events are not necessarily blooms, with high phytoplankton abundance or water discolouration. A bloom does not have to produce toxins to be harmful. Blooms can also deplete oxygen from water, block light to organisms or even clog or harm fish gills (Pitcher and Jacinto, 2019). For these reasons, harmful algal blooms (HABs) have become a major health and environmental concern worldwide (Anderson, 1995; He et al., 2020; Roselli et al., 2020; Zhang et al., 2020), especially for regions with aquaculture activities, where there is a direct impact in the economies and citizens. This is the case for the south of Chile, as this country occupies the second place in the worldwide production of several species of salmonfish (Fig. 1), with around 953.296 tons/year at the end of the year 2019 (Subpesca, 2019). An increase of the frequency and extension of algal blooms in the world's oceans has been confirmed by many authors (Anderson et al., 2012; Glibert et al., 2014; Gobler, 2020). This has also been the situation in Chile, where highly toxic HABs have become a serious problem for human health and the local economy (Lembeye, 2008). The triggers for bloom conditions are not fully understood, but nutrient enrichment of waters, especially by nitrogen and/or phosphates, as well as unusually warm conditions are recognized as precursors (Glibert and Burkholder, 2006; Klemas, 2012; León-Muñoz et al., 2018). With such diverse causes, prevention of HABs is difficult. Therefore, a more efficient technique of dealing with this threat is through an effective early warning system (Klemas, 2012; Sandoval et al., 2018).

Determining the species that form these blooms is key to assess their toxicity and damaging levels. In situ sampling is essential for this task. However, monitoring large areas using standard in situ techniques, as in the case of Chile, requires a large budget due to the costs of oceanographic logistic, equipment and sampling analysis in laboratories. For this reason, the programmes, in general, monitor a limited number of stations at strategic locations. During the last decades, the Government of Chile, as well as multiple public and private institutions, carried out intensive efforts to improve the sampling strategy and to coordinate the information collected at field (Sandoval et al., 2018). Some background information summarizing the history of red tide monitoring programmes and Institutions involved in Chile is described thereafter. The "Programa de Manejo y Monitoreo de las Mareas Rojas" conducted by the Fisheries Development Institute (IFOP), which has been in operation since 1994, is probably the oldest and more consistent monitoring programme in the country as well as one of the most ambitious in the world. IFOP's red-tide and environmental monitoring
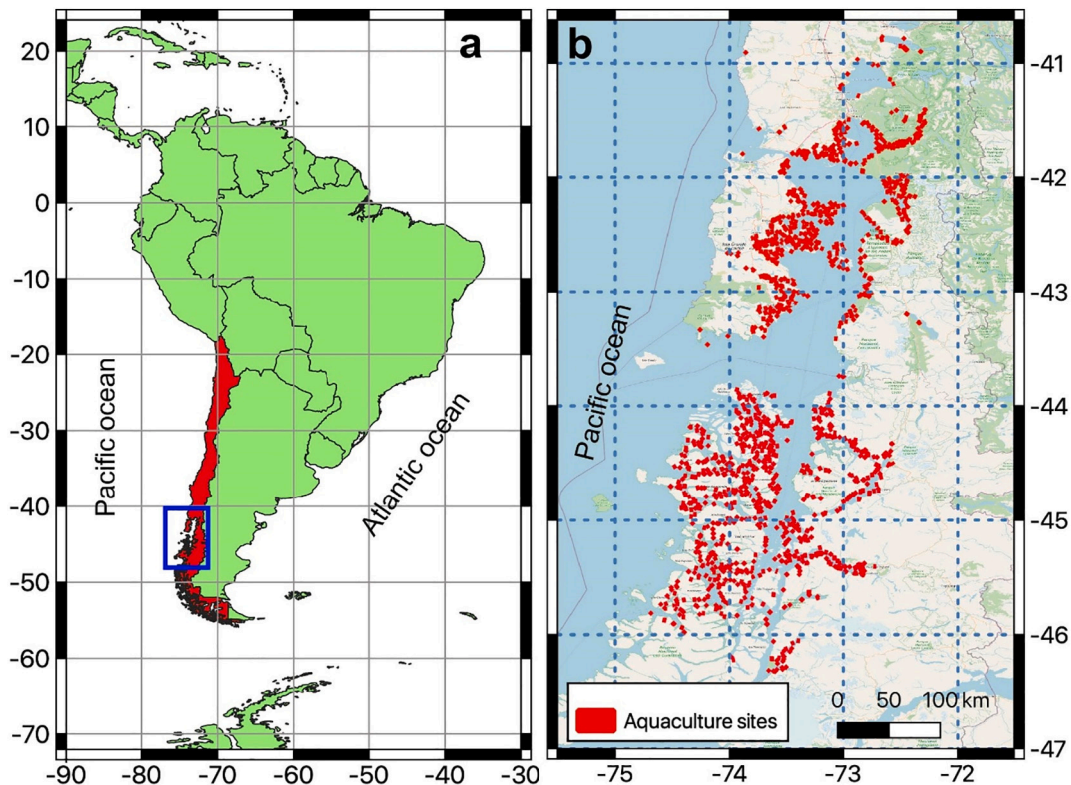
**Fig. 1.** a) General location of the study area in the coast of the Pacific Ocean, b) location of the aquaculture sites in this region of Chile.

is done on a monthly-basis in more than 200 stations across the entire Patagonian region, which, despite the large sampling and processing effort involved, is not always sufficient to provide an early warning of HABs events. There is also the "Programa de Sanidad de Moluscos Bivalvos" (Seaproduct Export Certification) of the "Servicio Nacional de Pesca" (SERNAPESCA) and the "Programa Nacional Integrado de Marea Roja" (audit sea products for national consumption) conducted by the Ministry of Health. In addition, the aquaculture industries managed by the Technical Institute of Salmonfish (Intesal) implemented the Phytoplankton Monitoring Programme (PROMOFI) to monitor the abundance and composition of phytoplankton. These monitoring systems cover the region of study; however, the strategies vary substantially in terms of number and location of sites and frequency of sampling according to the various objectives of each programme. Other programmes, such as the CIMAR - Fjords (CONA) programme, have focused on defining baseline conditions using synoptic surveys throughout the region. All the information is received by Sernapesca, the National Fisheries and Aquaculture Service (http://www.sernapesca.cl), for decision-making. The effectiveness of these monitoring systems depends on the spatial and temporal frequency of the in situ sampling. Nevertheless, it is also important to receive the samples in the laboratories as soon as possible. It is advisable to highlight that the reporting times of in situ monitoring efforts vary for each programme. As an example, PROMOFI is based on the collection and analysis of fresh samples of phytoplankton, and the deadlines for reporting results to fish farmers is usually less than 48 h from the time of sample collection, whereas in other programmes it takes longer (days to weeks). If, for some eventuality, the sampling is interrupted or the analyses are slowed down, difficulties will arise in decision-making leading to repercussions for health and productive activities. This was the situation occurred during the extensive algal bloom of *Cochlodinium* sp. and *Lepidodinium chlorophorum* (March–April 2020) in the southern coast of the Eastern Pacific at the latitudes of the Chilean Patagonia, as there was a temporal and spatial lack of information due to COVID-19 lockdown.

In this context, remote sensing might play a major role for monitoring this vast region, since data from space can assist the evaluation of relevant economic resources of areas at risk. Mueller (1979) first demonstrated the potential of remote sensing for HABs and this technology has been widely accepted for detecting and mapping algal blooms (Klemas, 2012). In the south of Chile, the first pilot and afterwards operational application of satellite sensors was carried out using ENVISAT (ENVironmental SATellite) data (Rodríguez-Benito and Haag, 2004; Rodríguez-Benito et al., 2006). The first results were related to total chlorophyll-a concentration (chl-a), which is the general indicator of the phytoplankton biomass (Parsons et al., 1985). However, this quantification is not as accurate as the use of other reflectance indices, as MERIS (MEdium Resolution Imaging Spectrometer) Chlorophyll Index (MCI) (Gower et al., 2008) or Fluorescence Line Height (FLH) for MODIS (Moderate-Resolution Imaging Spectroradiometer) (Gower et al., 2005), which were used during the monitoring of a massive algal bloom in this region during the austral summer of 2016 (Rodriguez-Benito and Haag, 2016). These indexes are based in the optical properties of the water and its constituents and were discussed by Gower (2016). New sensors like those from the Copernicus programme onboard Sentinel-2 (S2) and Sentinel-3 (S3) satellites allow better precision in detecting algal blooms due to the combination of higher spectral, temporal and spatial resolution. These sensors include reflectance bands designed to detect algal blooms (Ogashawara, 2019; Palenzuela et al., 2019; Caballero et al., 2020; Judice et al., 2020; Smith and Bernard, 2020). Different algal blooms absorb or reflect energy from different wavelengths in a unique way, thus providing the ability to identify their presence/absence (Dwivedi et al., 2015). Intensive efforts have been made in some countries to detect with satellites specific blooms of the two species evaluated in this research: *Cochlodinium* sp. (Noh et al., 2018) and *Lepidodinium chlorophorum* (Jegou, 2013; Morozov et al., 2013; Sourisseau et al., 2016).

The region of study in the coast of Chile is characterized by an archipelago of pristine waters with a multitude of channels, bays, fjords and islands, providing an ideal area for marine harvesting (Fig. 1).
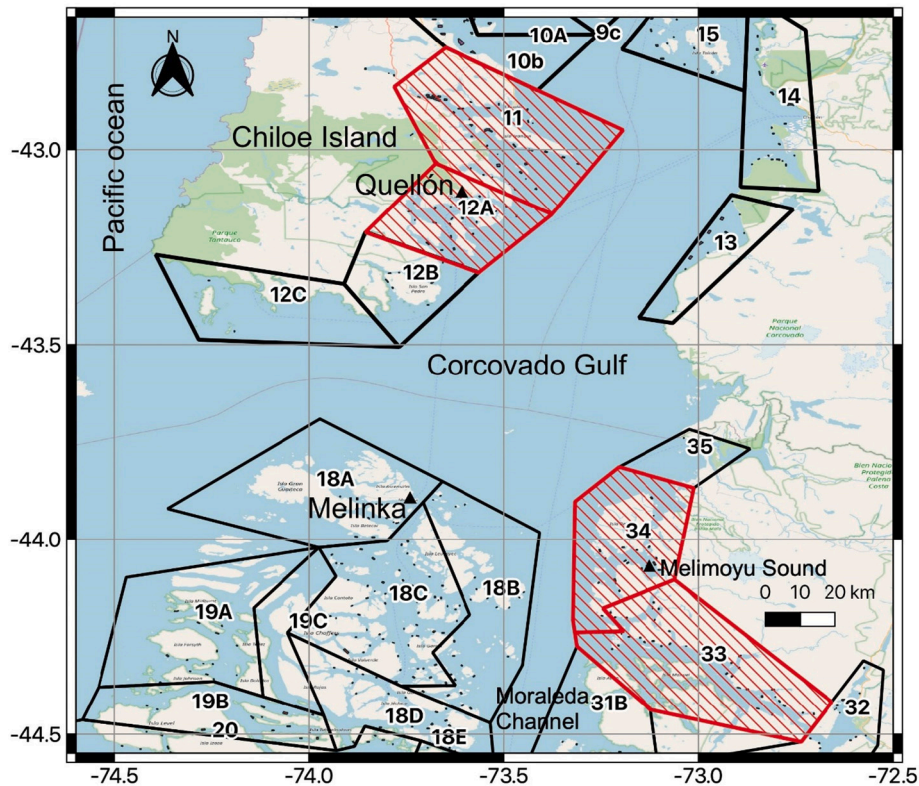
**Fig. 2.** Location of the selected case study sections (red areas), where mortalities in salmon farms occurred and were reported during the COVID-19 lockdown due to the harmful algal blooms monitored. (For interpretation of the references to colour in this figure legend, the reader is referred to the web version of this article.)

Since the beginning of the aquaculture activity in this region, HABs have caused mortality of farmed fish due to the presence of different phytoplankton species (Luxoro, 2018). None of these blooms caused the economic losses that occurred during the summer 2015–2016, when algal blooms occurred in the South Pacific along the Chilean coast mainly dominated by *Pseudochattonella verrucosa* (Clement et al., 2016; Rodriguez-Benito and Haag, 2016; Villanueva et al., 2016; León-Muñoz et al., 2018) and *Alexandrium catenella* (Armijo et al., 2020). The impact of this bloom drove the major socio-economic crisis on Chiloe Island, southern Chile, in 2016 (Mascareño et al., 2018). There has not been any human casualy, but the aquaculture insurance companies had their major losses in history (Anderson and Rensel, 2016). This large bloom was the reason for a massive mortality of salmon fish with losses around 800 million USD. Only satellite images allowed understanding of the magnitude and origin of this event, vaster that any other observed before. The information obtained through satellite remote sensing over strategic areas was given to decision-makers in the Public Health Secretary of the local Government (Rodriguez-Benito and Haag, 2016; Resolution 905, under the law 20.730/08-03-2014 of the Ministry of the Secretary General of the Presidency) to be used in the human health monitoring programmes, in combination with in situ data. In situ operational monitoring in open oceans is an impossible task for any government due to the available personnel and logistic limited budget. Conversely, remote sensing can detect massive blooms offshore, which can affect the coastal areas of the south of Chile, as it has been detected during the last 15 years (Rodríguez-Benito, 2019). As the best example we highlight the 2016 bloom mentioned before, which contained *Pseudochattonella verruculosa*, being responsible for the massive salmon mortality (León-Muñoz et al., 2018). Previous HABs events were also registered: in 1988, the first relevant losses of the industry were recorded due to a *Heterosigma akashivo* bloom (Díaz et al., 2019). A review of the blooms in the study area with more impact in the economic activities of the region was made by Luxoro (2018).

During March and April 2020, the Chilean aquaculture industry reported a massive mortality of salmon mainly due to the dinoflagellate *Cochlodinium* sp. (Mundo acuícola, 2020). The species detected were not harmful for the humans, but there were several taxa harmful for the salmon harvesting (Sernapesca, 2020). The fish mortality in the marine harvesting sites coincided with the declaration of the state of emergency in Chile due to the COVID-19 pandemic. The Ministry of Health of the Chilean Government declared the closure of roads to Chiloe Island (Resolution 203, 24th of March 2020 of the Ministry of Health in Chile. Document CVE 1744907), and the reduction of ship navigation in the area. Therefore, in situ sampling and sample transport to regional laboratories was slowed down inevitably. Due to the pandemic situation with the limitations imposed by the state of emergency, remote sensing of HABs events was a very powerful tool to monitor their temporal and spatial evolution and therefore, improve the management of this ecological crisis. However, cloudiness is a persistent problem in Southern Chile, which may represent significant challenges for blooms detection or water quality monitoring using satellite imagery. Cloud coverage data based on the observations from the meteorological station located in Tepual Airport, in Puerto Montt (Code 410005; 41.447° S; 73.095° W) belonging to the Meteorological Direction of Chile (https://climatologia.meteochile.gob.cl/) indicated the following statistics for the last annual 2019 report: 49% of days with severe cloud coverage, 11% of days with light cloud coverage and 40% of cloudless days. This aspect has been taken into account since ~40% of the satellite scenes thorough the study period (February–April 2020) had moderate to high cloud cover. Nevertheless, this circumstance has not limited the main objective of this research.

Accordingly, the purpose of this study was to monitor the detected algal blooms using the Copernicus medium and high spatial resolution satellites, S3 and S2, respectively, and evaluate their capability to map the location and extension of the HAB during the COVID-19 lockdown. Considering these bloom events as an example of salmonid aquaculture

impact during the COVID-19 lockdown in Chile, this research further indicates the benefit of the operational monitoring relying on Copernicus for improved coastal-management support in near real time (NRT).

## 2. Materials and methods

### 2.1. In situ data

In situ data regarding the phytoplankton species were obtained from official reports through the National Fisheries and Aquaculture Service public documents (http://www.sernapesca.cl), which collects all the information from the different regional public and private HABs monitoring programmes. This information is available periodically. We used Report 5 published on 24 April 2020 (Sernapesca, 2020), and some press released contemporary to the mortalities published in the beginning of April (Aqua Report, 7 April 2020; Aqua Report, 14 April 2020). The two regions evaluated in this study (Fig. 2) correspond to aquaculture sites where the salmon mortalities occurred due to the presence of high concentrations of the dinoflagellate species *Cochlodinium* sp. (which formally belongs to genus *Margalefidinium*, after Gómez et al., 2017). Other HAB species were also reported as *Lepidodiniun chlorophorum*, quantified with very high concentration, which caused water discolouration, but was not reported as responsible of fish mortalities.

One of the aquaculture sites affected by the bloom corresponds to the site "Tepun 102043" (SUBPESCA code), located in sector 12A by the Island Cailin at the south of the Chiloe Island (Fig. 2), where more than 15 tons of salmon were lost. The second case of study is located in sector 34 (Fig. 2), near Melimoyu Bay (in the eastern area of Corcovado Gulf), where at site "110899" losses of 43 tons of salmon were registered. The official information belongs to weeks 15–16 of the year (6–19 April 2020), two-three weeks after the detection of the blooms through remote sensing (Table 1). Information regarding mortalities was obtained from the official documents of Sernapesca (2020). For the *Cochlodinium* sp., the in situ samples indicated ~366 cells/ml in sector 34 on 12 April 2020, 580 cell/ml in sector 11 on 7 April 2020 and 25 cells/ml in sector 12A on 8 April 2020 (Table 1). In the reports of the industry to the Government, salmonid aquaculture companies have mentioned only losses higher than 15 tons, following the manual published in February 2017 by the Chilean Government (Sernapesca, 2017). These volumes of mortalities should be informed, as they require special logistics to treat the dead fishes and avoid environmental impact, which is audited by the authority to comply with environmental regulations. This means that, as mortalities < 15 tons should not be informed by the companies, the total amount of dead fishes would be different in a precise quantification.

### 2.2. Satellite data

S3 satellites from the Copernicus programme were used for NRT monitoring of the algal blooms. S3 is a mission comprising two satellites (S3A and S3B) in identical orbit with a phase shift of approximately 140°. S3A has been in orbit since February 2016, and S3B has been in orbit since April 2017; both satellites were operational at the time of the bloom and data from both constellations are available openly and freely for all users. The Ocean and Land Colour Instrument (OLCI)

**Table 1**
Information for the in situ data on *Cochlodinium* sp.
(Source: Sernapesca (2020).)

| Sector | cells/ml | Date |
|--------|----------|------------|
| 34 | 366 | 12-04-2020 |
| 11 | 580 | 07-04-2020 |
| 12A | 25 | 08-04-2020 |

**Table 2**
Specifications of the spectral bands of the satellite data used in this study: Sentinel-3 (300 m, daily revisit), Sentinel-2 (10–20–60 m, 5-day revisit), and Landsat-8 (15–30 m, 16-day revisit).

| Sentinel-3 | | Sentinel-2 | | Landsat-8 | |
|------|------------------|------|------------------------------------|------|------------------------------------|
| Band | Wavelength (nm) | Band | Wavelength (nm)/ spatial resolution (m) | Band | Wavelength (nm)/ spatial resolution (m) |
| 1 | 400 | 1 | 443/60 | 1 | 443/30 |
| 2 | 412.5 | 2 | 490/10 | 2 | 483/30 |
| 3 | 442.5 | 3 | 560/10 | 3 | 561/30 |
| 4 | 490 | 4 | 665/10 | 4 | 655/30 |
| 5 | 510 | 5 | 704/20 | 5 | 865/30 |
| 6 | 560 | 6 | 740/20 | 8 | 590/15 |
| 7 | 620 | 7 | 783/20 | | |
| 8 | 665 | 8 | 842/10 | | |
| 9 | 673 | 8a | 865/20 | | |
| 10 | 681 | | | | |
| 11 | 708 | | | | |
| 12 | 753 | | | | |
| 13 | 761 | | | | |
| 14 | 764 | | | | |
| 15 | 767 | | | | |
| 16 | 778 | | | | |
| 17 | 865 | | | | |
| 18 | 885 | | | | |
| 19 | 900 | | | | |

onboard S3 is a medium-resolution imaging spectrometer (300 m) with 14-bit radiometric resolution (ESA, 2019). It provides 21 bands (Table 2) and the revisit frequency is 1 day at the study region. Standard OLCI Level-2 Water Full Resolution (OL_2_WFR) products were downloaded from the EUMETSAT webpage (https://coda.eumetsat.int). Remote sensing reflectance corrected for the atmosphere and for sun specular reflection, hereinafter referred to as Rrs ($sr^{-1}$), in all visible and near infrared (NIR) bands was used. In addition, chl-a concentration was computed using two algorithms: the OC4Me algorithm, focused on open ocean Case 1 waters, in which phytoplankton is the main driver of water optical properties, and the neural network (NN) algorithm, particularly focused on more complex Case 2 waters, in which additional constituents must be considered such as scattering by total suspended matter or absorption by detrital and Gelbstoff material (ESA, 2019). Table 3 shows the S3 images selected. The main restrictions for this approach were associated with the relatively persistent cloudiness in the control area during the study period. Between February and April 2020–40% of the Sentinel scenes presented high cloud cover, restricting the information retrieved over the study region.

In addition, the S2 twin-satellite mission has been also evaluated for more details on coastal HABs monitoring due to its high spatial resolution (10–20–60 m, depending on the spectral bands; see Table 2) and open data access policy (ESA, 2015). The S2 mission, with a revisit frequency of 5 days, is based on a constellation of two identical satellites, in the same orbit, phased at 180° to each other. Both satellites were operational at the time of the algal bloom reported in this work. The radiometric resolution of the Multispectral Instrument (MSI) on board S2 is 12 bits, and the spectral characteristics of the bands used in this study are shown in Table 2. S2 scenes for the study area were downloaded from the Sentinel's Scientific Data Hub. These images corresponded to Level-1C (L1C) radiometrically and geometrically corrected Top Of Atmosphere (TOA) products (ESA, 2015). In this study, the images of zone 18 (subtiles GXS, GWS, GXT, GXR and GXU) were used. Only scenes with low cloud coverage over the study region were selected for further analysis (Table 3). Moreover, we also used Landsat-8 (L8) imagery for a detailed mapping of the algal bloom at a 30 m spatial resolution. These data are available from the Department of the Interior U.S. Geological Survey (USGS) and National Aeronautics and Space Administration (NASA). Landsat-8 acquires imagery of the

**Table 3**
List of imagery used in this study during the HAB events with minimum cloud coverage. Scenes from Sentinel-3 (S3), Sentinel-2 (S2), and Landsat-8 (L8) during February–April 2020.

| Date | Satellite | Image |
|------|-----------|-------|
| 2020/02/20 | Sentinel-3A | S3A_OL_2_WFR___20200220T135901 |
| 2020/03/25 | Sentinel-3B | S3B_OL_2_WFR___20200325T134112 |
| 2020/03/30 | Sentinel-3B | S3A_OL_2_WFR___20200330T135050 |
|  | Landsat8 | LC08_L1TP_233090_20200330_20200410_01_T1 |
| 2020/03/31 | Sentinel-3B | S3B_OL_2_WFR___20200331T142305 |
|  | Sentinel-2A | S2A_MSIL1C_20200331T142731_N0209_R053_T18GXS_20200331T175231, |
|  |  | S2A_MSIL1C_20200331T142731_N0209_R053_T18GXT_20200331T175231 |
| 2020/04/02 | Sentinel-3A | S3A_OL_2_WFR___20200402T141017 |
| 2020/04/08 | Sentinel-3B | S3B_OL_2_WFR___20200408T141536 |
|  | Landsat8 | LC08_L1TP_232089_20200408_20200408_01_RT, LC08_L1TP_232090_20200408_20200408_01_RT, LC08_L1TP_232091_20200408_20200408_01_RT |
|  | Sentinel-2B | S2B_MSIL1C_20200408T143729_N0209_R096_T18GXS_20200408T193410, |
|  |  | S2B_MSIL1C_20200408T143729_N0209_R096_T18GXT_20200408T193410, |
|  |  | S2B_MSIL1C_20200408T143729_N0209_R096_T18GWS_20200408T193410 |
| 2020/04/11 | Sentinel-3A | S3A_OL_2_WFR___20200411T133939 |
| 2020/04/30 | Sentinel-3A | S3A_OL_2_WFR___20200430T134710 |

Earth's terrestrial and polar regions in the visible, NIR, short wave, and thermal infrared spectra with a 16-day revisit frequency (Knight and Kvaran, 2014). The Operational Land Imager (OLI) sensor has enhanced spectral characteristics compared to the Landsat 7 Enhanced Thematic Mapper plus (ETM +), and includes an improved signal-to-noise ratio and 12-bit radiometric resolution (Woodcock et al., 2008). Orthorectified and terrain corrected Level 1 images were downloaded from Earth Explorer (https://earthexplorer.usgs.gov/). The tiles corresponding to the region of interest were in paths 232/233 and rows 89, 90 and 91 (see Table 3 for acquisition dates).

All the L8 and S2 Level-1 images were atmospherically corrected to Level-2A (bottom of atmosphere, BOA) with the ACOLITE processor (version 20190326.0, https://odnature.naturalsciences.be/remsem/software-and-data/acolite). ACOLITE programme uses an image-based approach that does not require in situ atmospheric information. ACOLITE was specifically developed for marine, coastal and inland waters by the Royal Belgian Institute of Natural Sciences (RBINS) and supports free processing of both L8 and S2 (Vanhellemont and Ruddick, 2016). We selected a novel algorithm within the ACOLITE toolbox, the Dark Spectrum Fitting (DSF) atmospheric correction model (Vanhellemont and Ruddick, 2018; Vanhellemont, 2019). This recent algorithm was initially developed for water applications of metre-scale optical satellites but has already indicated its potential for application to S2 due to their improved spectral coverage, notably including bands in the short wave infrared region (SWIR) (Vanhellemont, 2019). In this study, we also selected this algorithm with the optional image-based sun glint correction of the surface reflectance. ACOLITE products correspond to Rrs in all visible and NIR bands, resampled to 10 m pixel size for S2 and 30 m for L8. The chl-a concentration was also generated using the OC3 algorithm, a three banded maximum band ratio that uses fourth order polynomial function, for S2 and L8 as a proxy of the bloom extent (Vanhellemont, 2019).

### 2.3. Normalized difference chlorophyll index (NDCI)

We have applied the normalized difference chlorophyll index (NDCI, Eq. (1)), described by Mishra and Mishra (2012), which uses the red and red-edge band. The red-edge band is designed to capture the reflectance in the red/far-red wavelength. In this area of the spectra and due to the optical properties of both the water and the phytoplankton, it is possible to obtain higher sensitivity of HABs in respect with the classical blue/green ratio. This is achievable due to the sum of several facts previously explained by Noh et al. (2018), specifically for *Cochlodinium* sp. and similar species, which are the fluorescence emission, the pigment absorption at around 660 nm, the strong water absorption at above 700 nm and the backscattering of biological particles in the red

and NIR wavelength. Following Gower et al. (2005) and Gower (2016), the center wavelength of the red edge like peak migrates towards 710 nm as chlorophyll *a* concentration increases. NDCI uses the bands at 665 nm (Rrs665) and 708 nm (Rrs708) emulating the MERIS channels and the reflectance peak centered at 700 nm, which is maximally sensitive to the variations in chl-a concentration in water. This avoids the confounding influence of Coloured Dissolved Organic Matter (CDOM) and total suspended sediments in the water reflectance at shorter wavelengths. Both S3 (band 8 and band 11) and S2 (band 4 and band 5) have specific bands for determining the NDCI, whereas L8 only has the red band (Table 2). Therefore, the NDCI was only established for the Sentinel satellites. Following the recommendation of Noh et al. (2018), NDCI values higher than zero were highlighted as an indicator of the algal bloom in the Corcovado Gulf and adjacent areas.

$$\text{NDCI} = \frac{Rrs708 - Rrs665}{Rrs708 + Rrs665} \text{ (dll)}$$
(1)

## 3. Results

### 3.1. Near real time monitoring with Sentinel-3 imagery

The evolution and distribution of the algal bloom during the COVID-19 quarantine period was monitored using daily S3 NRT data at 300 m spatial resolution. The first areas affected by the bloom were located in the South of Chiloe Island and in the southeast zones of the Corcovado Gulf (Sernapesca, 2020). These areas correspond to the administrative aquaculture sections 11, 12A and 34 (Fig. 2). The maps of chl-a calculated with the standard OC4Me and NN algorithms are displayed in Figs. 3 and 4, respectively. The days were selected based on minimal cloud coverage (Table 3). For the OC4Me algorithm, there were some regions inside the bloom and along the coast that were masked out, whereas the NN algorithm provided information over coastal regions and over the bloom areas (applying the standard flagging for each algorithm described in EUMETSAT, 2018). OC4Me showed higher concentrations compared with NN and both algorithms indicated higher chl-a concentrations on 31 March, 2 and 8 April 2020, coinciding with days when fish mortality was reported by the aquaculture companies to the authorities (Sernapesca, 2020). Chl-a is a traditional proxy for blooms extension and biomass. However, in this case, it did not perform properly on delineating the spatio-temporal variability of the HABs.

In order to overcome this issue, we used NDCI for the same dates as chl-a (Fig. 5). In this case, the spatio-temporal evolution of the bloom over the entire Corcovado Gulf was clearly indicated applying this index with values > 0. At the end of February some positive values were detected in the South of Chiloe and around Melinka Island (northern and southern areas of this Gulf), following the map on 20
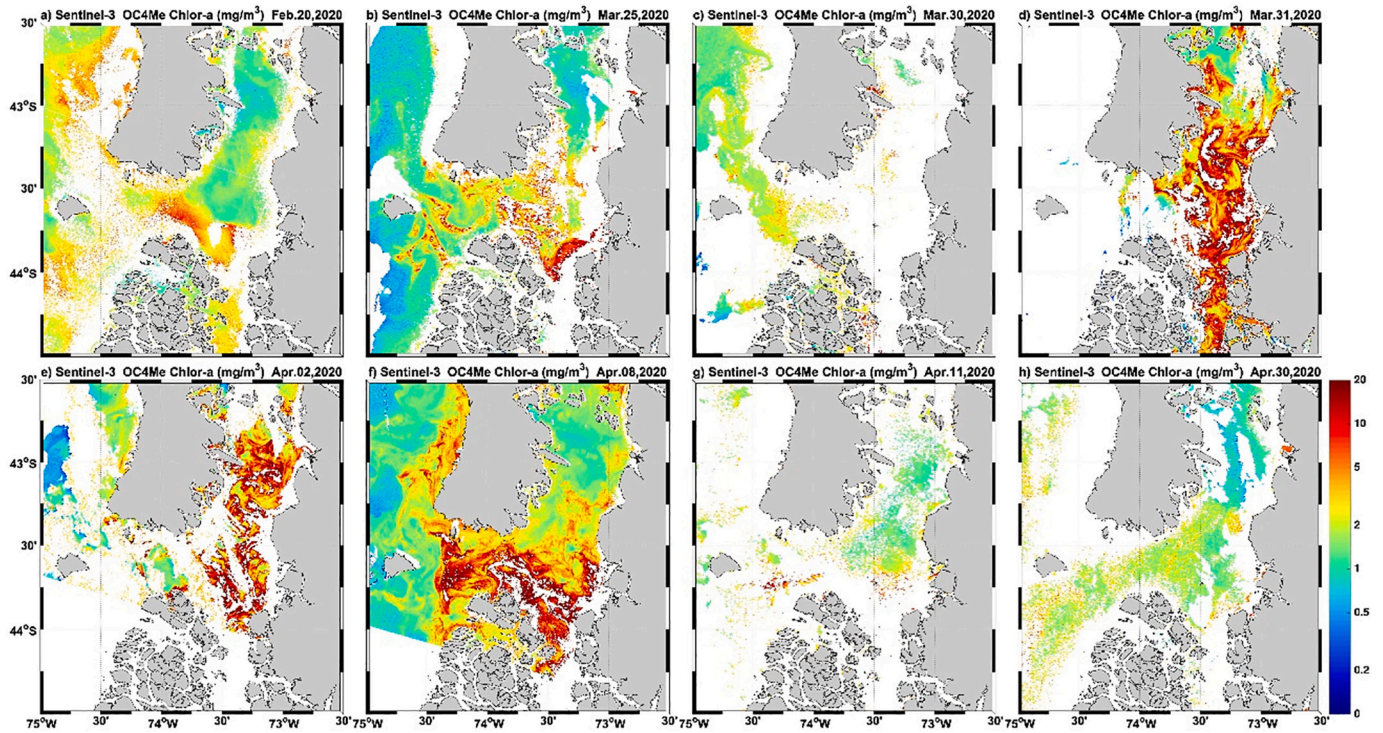
**Fig. 3.** Temporal evolution of the phytoplankton chlorophyll concentration in the area of study in Chile during February–April 2020 from S3 at 300 m spatial resolution. Chlorophyll concentration computed through the OC4Me algorithm (Chlor-a).

February 2020. The bloom was extending along the next weeks towards March 25, but particularly on 30–31 March 2020, extensive bloom features can be detected with the NDCI, indicating that the bloom covered the total study region with heterogeneous patches. The most frequently occurring NDCI values varied from 0 to 0.7, with some regions peaking at 0.8–0.9 values, implying a moderately high bloom condition. On 8 April 2020 the algal bloom was confined to the southern region of the Corcovado Gulf, clearly impacting areas of the Moraleda channel. From 11 April 2020, the bloom diminished and on 30 April images were characterized by minimal chl-a concentrations and lower NDCI values. Several days after 30 April were also evaluated with S3 data, but no bloom was visible. These findings suggest NDCI is a
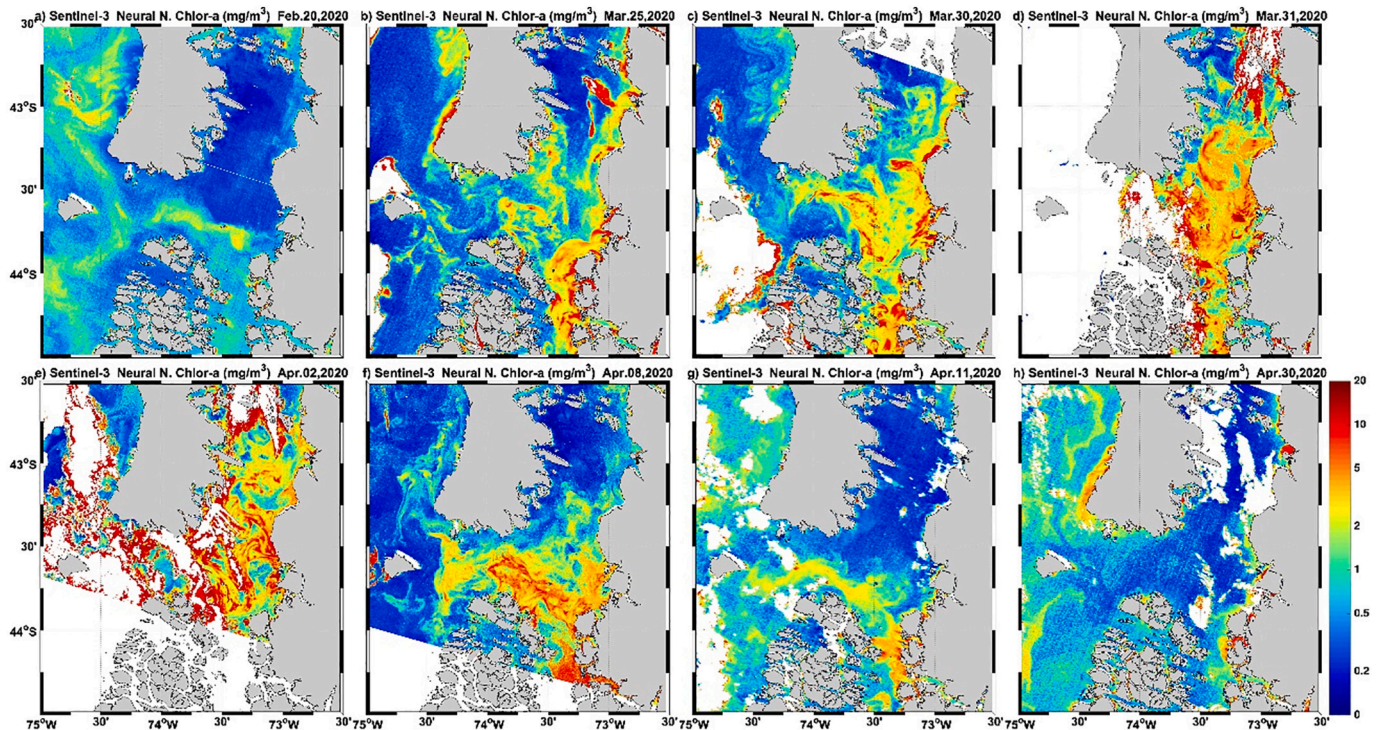


**Fig. 4.** Temporal evolution of the phytoplankton chlorophyll concentration in the area of study in Chile during February–April 2020 from S3 at 300 m spatial resolution. Chlorophyll computed through the Neural Network algorithm (Chlor-a).
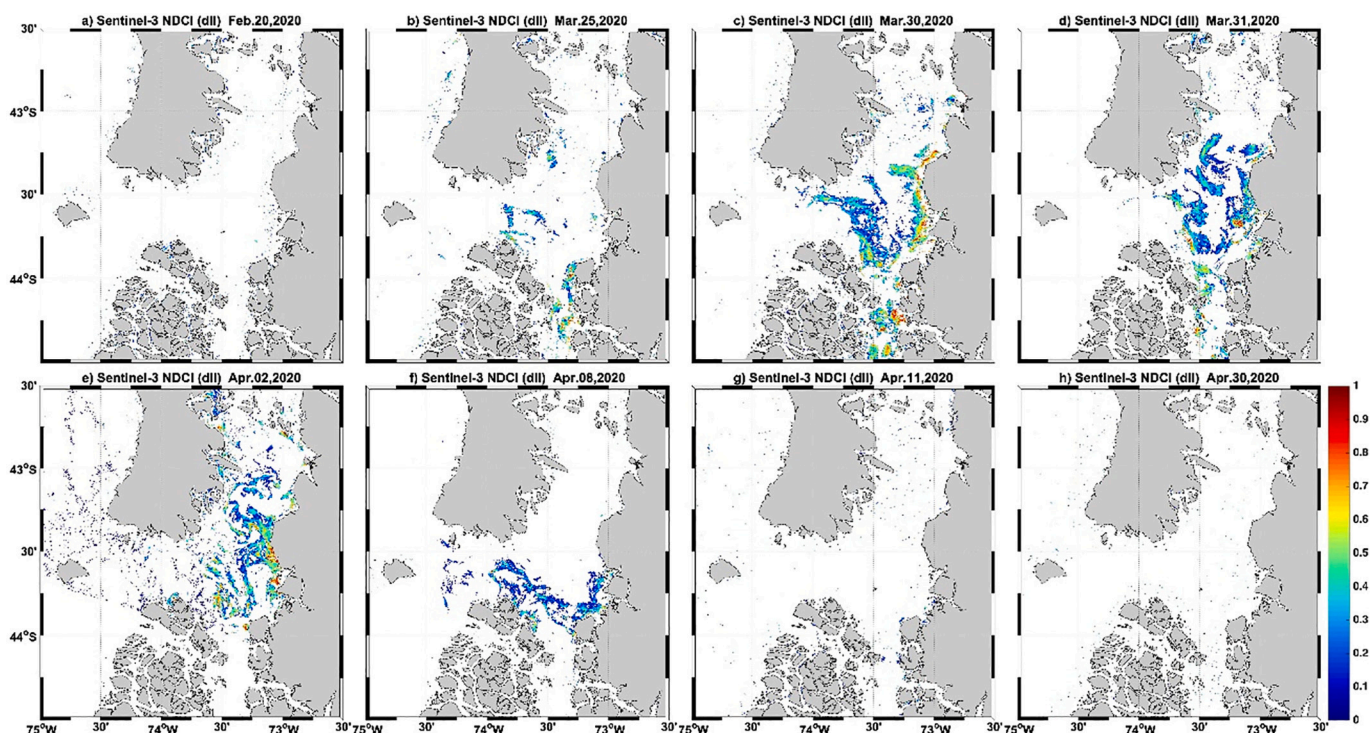
**Fig. 5.** Temporal evolution of the algal bloom using the normalized difference chlorophyll index (NDCI) from S3 imagery during February–April 2020. Only positive NDCI values indicating bloom area are displayed.

good proxy for the HABs occurring over the study area. The results were also similar to in situ observations on the events of fish mortalities starting at the end of March 2020; with first areas affected by the bloom located in the south of Chiloe Island, and in the southeast areas towards the continental region of the Corcovado Gulf (administrative aquaculture sections 11, 12A and 34, Fig. 2) (Sernapesca, 2020). Even though in situ sampling was slowed down during this period due to the COVID-19 lockdown, the S3 products allowed us to continue observing in NRT the development of blooms and their severity over this complex and vast region. This information is a clue for a better allocation of in situ monitoring purposes by the aquaculture companies and for the regional Government with high impact on several salmon production areas, as those mentioned here.

For a detailed evaluation of the events of fish mortalities with S3 in the study area, South of Chiloe Island, Fig. 6 show the RGB composite, the distribution of chl-a NN, the remote sensing reflectance at 708 nm (Band 11) and the NDCI on 31 March and 8 April 2020. The algal bloom can be clearly recognized by a discolouration of the water, manifested as intensely green and brownish coloured water, on 31 March close to Quellón (administrative aquaculture sections 11 and 12A, Fig. 2) and on 8 April close to the Melimoyu region (administrative aquaculture section 34, Fig. 2). Whereas the chl-a NN concentration indicated high values for both days over the entire study region, the NDCI maps depicted the bloom extent thoroughly. The identification of the pixels and the severity of the bloom was calculated with the NDCI mask (NDCI > 0 to 1). Moreover, the Rrs at 708 nm map (the red-edge band used for the NDCI), suggests it is a good proxy for bloom monitoring, indicating the maximum bloom coverage on 31 March 2020, where the patchiness of the bloom was spread over the study area from offshore to coastal areas. These bloom patterns were in accordance with the in situ observations shown in Table 1 (Sernapesca, 2020), highlighting a peak of the bloom on 30–31 March 2020 as opposed to the confined bloom areas on 25 March and previous days. This bloom was produced mainly by *Cochlodinium polykrikoides*, which presents a strong spectral peak at around 700 nm as described by Noh et al. (2018). In order to illustrate how the red-edge band at 708 nm can capture the reflectance peak of

the bloom, Fig. 7 shows the reflectance spectrum for 3000 random pixels within the study area corresponding to Fig. 6 for S3 scenes acquired on 31 March and 8 April 2020, as well as the histogram of NDCI and the corresponding chl-a NN values. The peak at 708 nm became more pronounced as NDCI increased from 0 to 0.25 (Fig. 7e and f), 0.25–0.5 (Fig. 7g and h), and 0.5–1 (Fig. 7i and j) values, displaying similar patterns for both scenes. For the latest, higher reflectance at 708 nm band were observed compared with those of the green band at 560 nm, suggesting the center wavelength of the green peak migrated towards the red-edge 708 nm as chlorophyll concentration and biomass of the algal bloom increased.

### 3.2. Monitoring with high-resolution imagery: Sentinel-2 and Landsat-8 satellites

This study also aimed at evaluating the spectral capabilities of the S2 imagery for monitoring HABs in this region. For that aspect, we analyzed the spectral signature of S2 compared with S3. Fig. 8 shows the reflectance along the visible and NIR bands in some locations of S3 (1 pixel, 300 m) and S2 (15 × 15 pixel of 10 m box centered at the S3 location) images acquired on 8 April 2020. The true colour composite indicates an algal bloom that gave the water a green hue comparable to that of terrestrial vegetation. Brownish areas were also observed mixed with the green patches. The S2 spectral signal was obtained after atmospheric and sun glint correction with ACOLITE DSF. Four control points were selected based on the NDCI values: three of them were inside the algal bloom (P1, P2 and P4) whereas P3 was outside the bloom. First, it is worth mentioning that the Level 2 bottom of atmosphere (BOA) reflectance indicated that the atmospheric and sun glint corrections with ACOLITE performed accurately, with a signature comparable along the visible and NIR spectra for both satellites. Moreover, the additional red-edge bands of S2 (704, 740, and 783 nm; Table 2) were able to provide information about the bloom, specifically the 704 nm band, which is the one used for NDCI calculation. The peak at 708 nm noted with S3 for the points inside the bloom was also visible in the 704 nm band with S2, particularly in P1 and P4. Using both
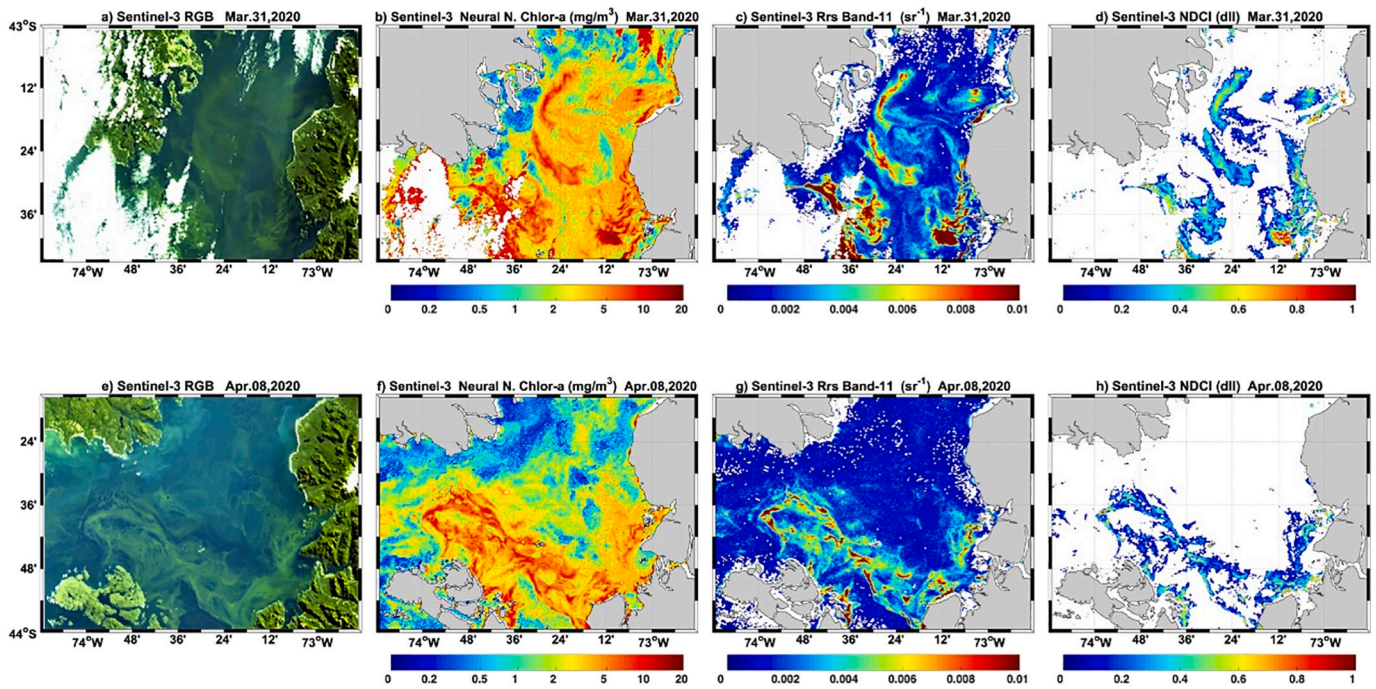
**Fig. 6.** a) RGB (red-green-blue) composite, b) distribution of chlorophyll concentration (Neural Network algorithm), c) remote sensing reflectance at band 11 (708 nm), and d) normalized difference chlorophyll index (NDCI) from a S3 image acquired on 31 March 2020; e–h) the same from a S3 image acquired on 8 April 2020. (For interpretation of the references to colour in this figure legend, the reader is referred to the web version of this article.)

resolutions, operational in the first case with S3 and local in the second with S2, the reflectance shows a clear peak in the red edge (704–708 nm), confirming the presence of the bloom. In addition, the NDCI values calculated with both satellites were similar or equal in some cases: P1 is 0.59 and 0.55 for S3 and S2; P2 is 0.1 and 0.1 for S3 and S2; P3 is −0.14 and −0.12 for S3 and S2; and P4 is 0.54 and 0.42 for S3 and S2, respectively. These results confirm that both red-edge bands 708 nm and 704 nm were a clue for masking the algal bloom with the NDCI. S2 is a suitable option for a detailed mapping of the HAB in this coastal region.

The operational monitoring was carried out with S3 data (Figs. 3–6), as it can be used for NRT mapping. Nevertheless, RGB composites and NDCI maps were generated using S2 (Fig. 9) to get a detailed inspection of the bloom corresponding to the areas where the farms reported mortalities of salmon fishes (sector 12A, by the Cailin Island, and sector 34, near Melimoyu Sound; Fig. 2). Similar bloom patterns were observed with both satellites, noting the different spatial resolutions of S2 at 10 m (Fig. 10) and S3 at 300 m (Fig. 6). Even if S3 is able to detect the bloom at mesoscale, S2 allows a better visualization and mapping of the heterogeneous bloom by using NDCI values > 0. For inland waters and regions with complex geomorphology, as in this case, the potential of S2 to map the bloom at 10 m needs to be highlighted. Many S3 pixels were masked out and excluded due to land/water interference and other artefacts, while S2 offered a complete identification of the bloom. Compared with that of the S3 image, the higher spatial resolution of the MSI image revealed intense small patches of the bloom close to both aquaculture sections 12A and 34 on 31 March and 8 April 2020, respectively.

Landsat-8 satellite at 30 m spatial resolution was also examined for an enhanced spatial monitoring of the bloom. The spectral features are clearly observed from two S2 and L8 scenes on 30–31 March and 8 April 2020 in the two study areas, Cailin Island (Fig. 10a and b) and Melimoyu Bay (Fig. 10c and d), respectively. A comparison of pixels with high NDCI (calculated from S2), such as P1 and P2 (0.25 and 0.34 in section 12A, 0.57 and 0.45 in section 34), indicates L8 is able to capture the green peak similarly to S2. However, the peaked reflectance of the

704 nm band in both regions captured by S2 is a preferable advantage compared to the spectral characteristics of L8, which are limited within this red-edge part of the spectrum. In contrast, for P3 and P4 with low NDCI varying from 0.01 to 0.1, similar reflectance values were contained for both satellites. Therefore, the distinct optical signature of S2/S3 compared with that of L8 implies that L8 lacked the necessary optical feature along the red-edge to map these blooms with NDCI. An example of a L8 scene acquired on 30 March during the first mortality event reported in the harvesting section of Quellón-12A is displayed (Fig. 11). The RGB composite at BOA level (after ACOLITE atmospheric correction) and the map of chl-a concentration peaking in the bloom area were similar to S3 imagery on 30 March 2020 (Fig. 11). A zoom on the 12A section showing high chl-a concentration over the salmon farming area recording fish mortality on 30 March 2020 is also shown (Fig. 11c).

## 4. Discussion

This study demonstrates the operational capabilities of the optical satellites from the Copernicus programme. The tools implemented using S3 and S2 imagery allowed monitoring of the extension and severity of the HABs occurred in the southern coast of Chile during the COVID-19 lockdown (March–April 2020). The COVID-19 pandemic is changing not only many aspects of our way of living but also indirect effects in the environment have been already described, as the reduction of atmospheric pollution due to the interruption of the citizen mobilization (Zambrano-Monserrate et al., 2020) or regarding the improvement of the water quality in lakes as demonstrated by Yunus et al. (2020). The pandemic situation affects the logistics around the world in many aspects during the lockdown, as in this case study regarding local phytoplankton monitoring programmes. Local samplings from the regional monitoring programme were slowed down or cancelled due to the confinement. However, Copernicus images allowed observation of the algal bloom except when scenes were cloudy (40% of time), and therefore, to advice the authorities on time to be prepared for possible massive salmon mortality events on the aquaculture sites. This helped
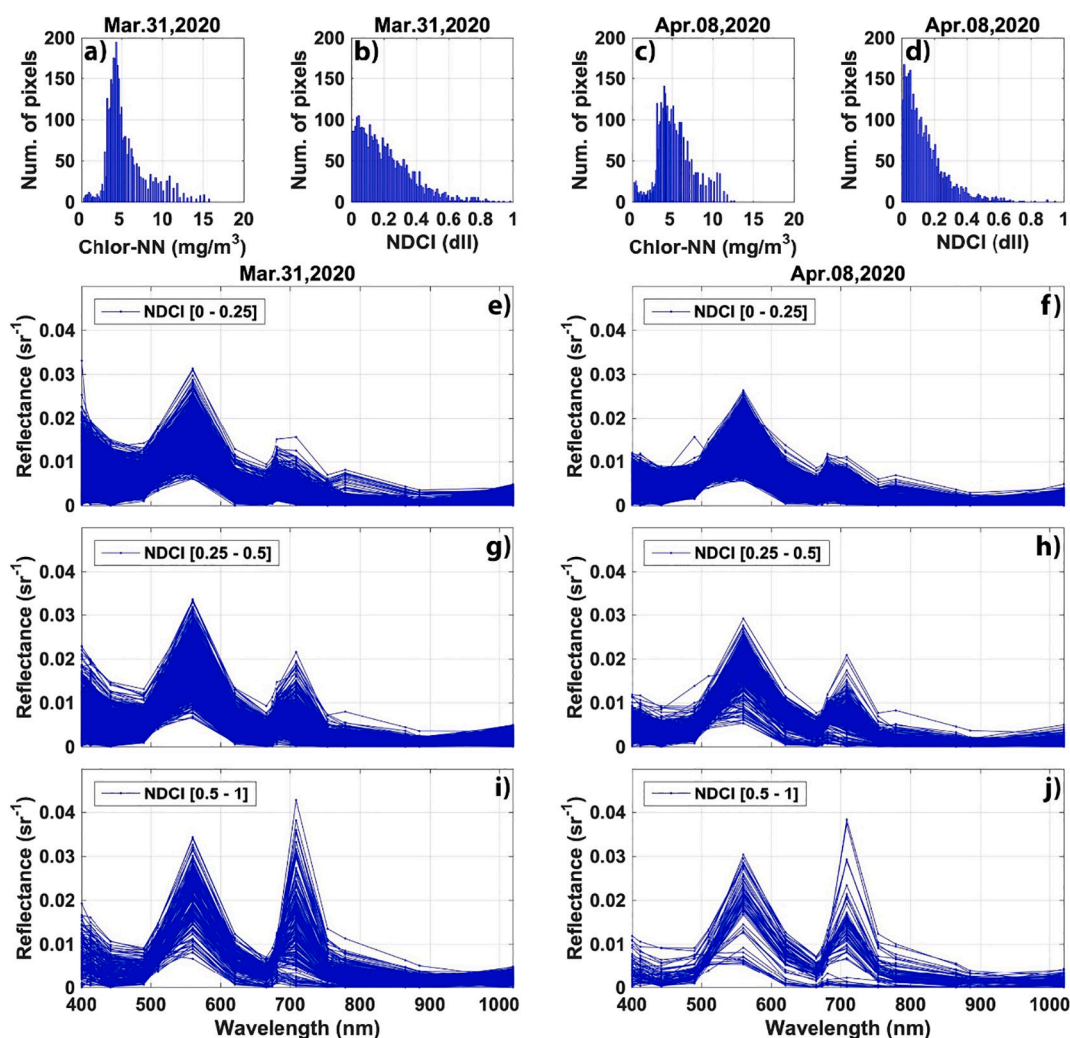
**Fig. 7.** Histograms of chlorophyll concentration (a, c) and normalized difference chlorophyll index (NDCI)(b, d) for the study area (Fig. 6) on 31 March and 8 April 2020, respectively, from S3; (e–i) reflectance spectra over 3000 randomly selected pixels with positive NDCI values on 31 March 2020, f–j) the same on 8 April 2020.

to avoid major socio-economic impacts, as occurred in previous events. Fish farming is the third largest economic activity in this country (Cerda, 2019). Therefore, all the relevant information on its aspect is of benefit for both Government management and citizens. This is a global issue, which further underlines the international relevance of this type of studies.

In this region, different major red tide species are responsible for annual blooms between spring and autumn periods. A review of the blooms with more impact in the economic activities of the region was made by Luxoro (2018). Mardones and Clement (2016) described in their guide the main harmful species detected in the south of Chile. Therefore, timely mapping of widespread HAB distribution in this coastal area is decisive in minimizing the damage and evaluating the environmental impacts of bloom events. During last years, there was an increase of economic support to improve scientific tools in order to help in the early alarm systems. This was specially enhanced after the extreme salmon mortalities occurred during 2016, when millions of USD losses were reported by the aquaculture companies and supported by the insurance companies (Rodriguez-Benito and Haag, 2016; León-Muñoz et al., 2018). The most intense and extensive blooms have been observed to be originated offshore. The main connection with the open ocean is the Gulf of Corcovado where the current direction is aligned with the channel axis (Castillo and Velenzuela, 2008). These authors described the currents and their patterns as a response to tidal forcing, geostrophic circulation and variations of local wind field (Cáceres et al.,

2002; Cáceres et al., 2003). The spatial evolution of the bloom observed in this study fits well with the local oceanographic circulation described by these authors. These oceanographic dynamics could explain the origin and evolution of the observed bloom in 2020 and will be object of future research to determine its main environmental drivers.

Our findings suggest chl-a OC4Me and NN algorithms were not enough information to monitor the bloom distribution with S3 in these complex regions. The results from preliminary validations of S3 algal pigment concentrations have suggested OC4Me underestimates in oligotrophic waters whereas better results were found in meso- and eutrophic waters (Kwiatkowska, 2018). ESA and Copernicus are planning an algorithm update in the future. Some recent works have also suggested there is not significant correlation for the OC4Me algorithm with in situ observations in the Mediterranean Sea (Moutzouris-Sidiris et al., 2019) and in the South China Sea (Han et al., 2019). Therefore, we proposed the reflectance-based algorithm NDCI product from S3 for daily NRT monitoring of the HABs, as the first approach in the operational actions. This tool would be especially useful for the regional monitoring programme, for an early-stage alert on blooms and for mapping the spatiotemporal variability at better resolution (300 m) than other standard ocean colour sensors such as MODIS at 1 km (Lara et al., 2017) or the Visible Infrared Imaging Radiometer Suite (VIIRS) at 750 m.

The NDCI algorithm for both S2 and S3 can provide reliable and relevant information in quasi-real time to prepare for and respond to
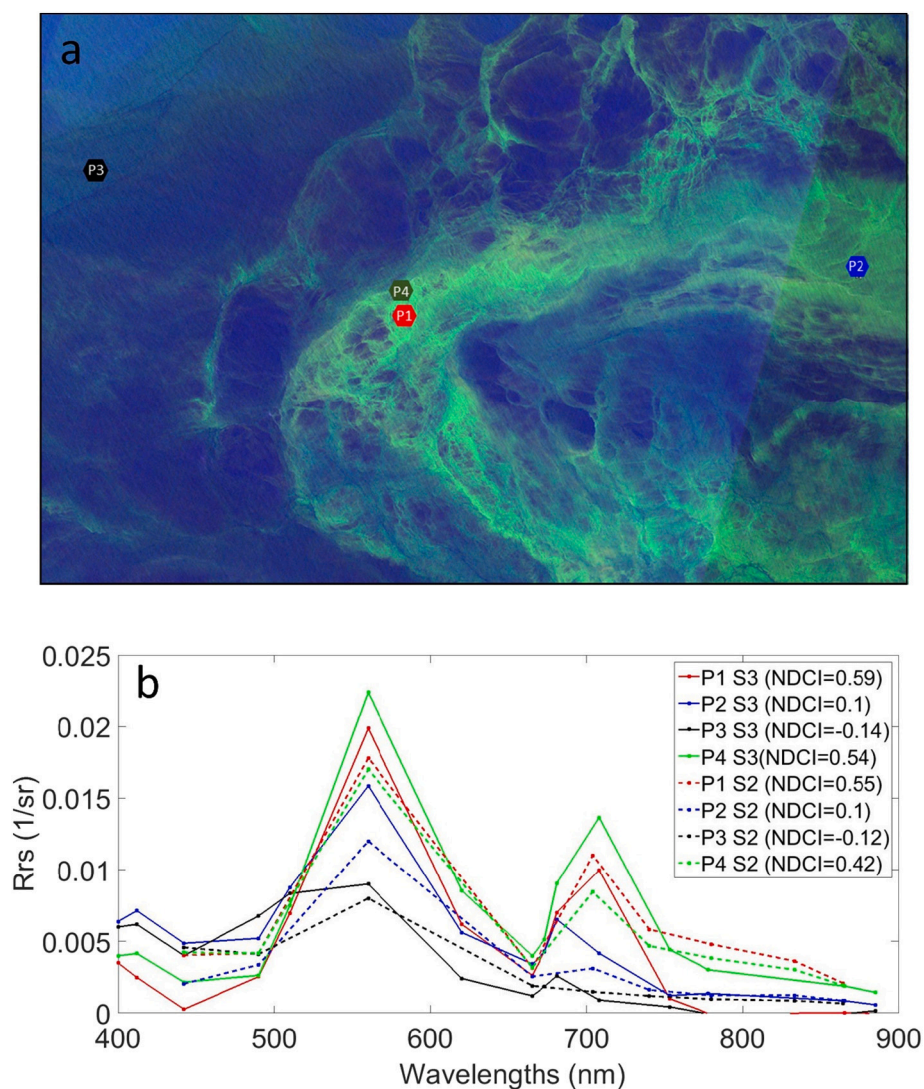
**Fig. 8.** a) RGB (red-green-blue) composite from a S3 scene acquired on 8 April 2020, b) Spectral signature in some pixels (P1, P2, P3, and P4) of the scene from S3 (300m) and S2 (15 × 15 pixel box centered at the S3 location) on 8 April 2020. The normalized difference chlorophyll index (NDCI) values are indicated for each pixel and satellite (S3 and S2). (For interpretation of the references to colour in this figure legend, the reader is referred to the web version of this article.)

red tides as well as for determining the bloom distribution during the event. The specifications of the S3 and S2 Copernicus' missions were analyzed, as well as the spectral features obtained from both satellites. S3 in an operational way and S2 with local resolution are adequate tools for algal bloom monitoring. Advantages and drawbacks of each sensor have been mentioned and should be considered when incorporating these tools formally in the future monitoring procedures. Operational surveillance can be made using S3, at mesoscale. Then, in case of positive values of the NDCI index, even in cases of a small size of the patches in the beginning of an algal bloom, S2 data could be used to increase the spatial resolution and give precise information of the location of the bloom for early-alarm system to the harvesting companies at local scales. This is especially relevant to resolve features in narrow areas such as the fjords and channels where aquaculture sites are located along the south of the Chilean coast. S2 imagery allowed a fine-scale delimitation of bloom patches, even during the beginning of a bloom, which helped to alert to decision-makers about the potential impact of HABs. This simple algal bloom mapping strategy can be used, in combination with standard in situ observations, to control and manage HABs in fjords, channels and protected areas of Patagonia.

Phytoplankton biomass and especially algal blooms in coastal, estuarine and inland water environments are frequently inferred from the shape of the visible and NIR spectra obtained from remote sensing observations. The spectral curves in this study show that the pixels inside the algal bloom often exhibited acute reflectance peaks in the red-edge bands at 708 nm and 704 nm, for S3 and S2, respectively. The bloom studied in this work covers an event with the presence of the dinoflagellates *Cochlodinium polykrikoides*, one of the species responsible for the salmon mortalities (Sernapesca, 2020). The reflectance response of this species of phytoplankton has been described by other authors (Son et al., 2011; Noh et al., 2018) with a clear reflectance peak at 678 nm in the near infrared part of the spectra when red tide was present, due to the high phytoplankton concentration of these species. Minimum values were encountered for non-bloom pixels. Similar reflective spectra in the red-edge bands have also been observed by several researchers and have usually been associated with algal blooms (Gower et al., 2005; Gower et al., 2008; Hunter et al., 2010; Toming et al., 2016; Molkov et al., 2019). Kim et al. (2016) carried out an optical discrimination of *Cochlodinium polykrikoides* in Korean waters, through the spectral response of the algae, using the same criteria. The prominent reflectance peak located in the 700–720 nm region shifts towards longer wavelengths as phytoplankton concentrations increase; thus, these bands are suggested as the best option for HABs mapping (Toming et al., 2016). Sakuno et al. (2019) already indicated the
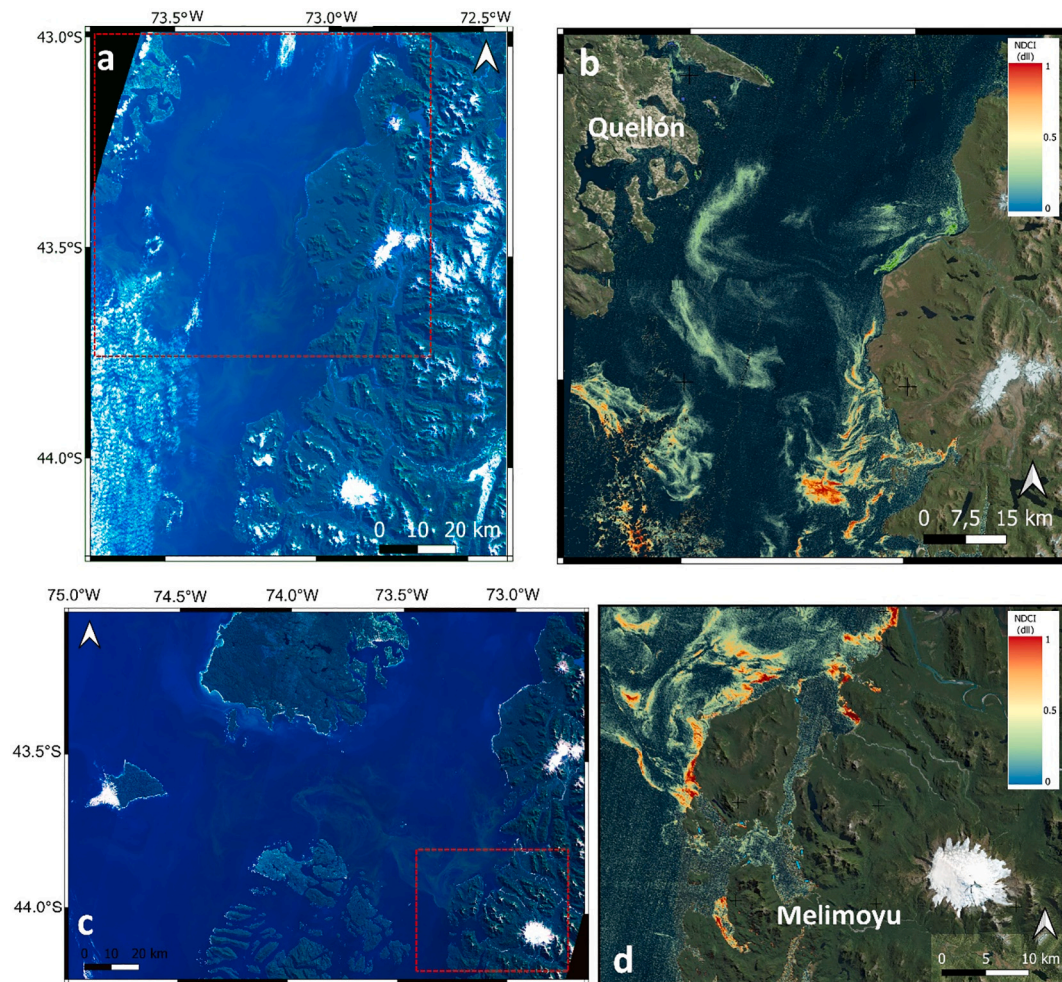
**Fig. 9.** a) RGB (red-green-blue) composite and b) normalized difference chlorophyll index (NDCI) map of S2 at 10 m for the salmon sections where fishes mortalities were reported during the bloom monitored in this study on 31 March 2020 in Cailin Island, c, d) the same on 8 April 2020 in Melimoyu bay. (For interpretation of the references to colour in this figure legend, the reader is referred to the web version of this article.)

potential of the 704 nm red-edge band of S2 for red tide monitoring in Japan. The sensitivity of NDCI to chl-a concentration in turbid productive waters has been demonstrated, as well as its potential application to several platforms and diverse environments, producing minimal uncertainty (Mishra and Mishra, 2012). As the red-edge bands of S2 and S3 are required for the calculation of NDCI, both missions allow the monitoring of algal blooms in optically complex and productive estuarine and coastal waters such as those in this coastal study region, with freshwater input from the fjords and influenced by open ocean waters. The reflectance spectra also presented an intense signal in the green wavelength, which could be the response of the abundance of the *Lepidodinium chlorophorum* species, also detected in the in situ samples (Sernapesca, 2020). The patterns observed in the radiance spectra fit well with the response of this species as Jegou (2013) and Sourisseau et al. (2016) showed along the French Atlantic shelf and Morozov et al. (2013) showed along the Bay of Biscay. Therefore, we suggest that these results represent the reflectance response of both main species detected from in situ data.

Since the early 1990s, ocean temperatures have increased as well as blooms of the ichthyotoxic dinoflagellate *Cochlodinium polykrikoides* in the northern hemisphere (Griffith et al., 2019). Onitsuka et al. (2010) mentioned an expansion of the same species in western Japan and southern Korea over the last two decades. Cortes et al. (2019) presented the state of knowledge of this species in Latin America, but there is not any mention for Chile. In our study area, the species was previously detected by Mardones and Clement (2016), but not with any harmful

consequences for the regional aquaculture. Therefore, this event could be the first one with negative repercussions for the salmonid farming industry. The global warming tendency measured around our planet suggests that its effect in the southern hemisphere could also increase the number of events and abundance and geographical expansion of some harmful species (Gobler, 2020), as those mentioned in this study. In this sense, operational monitoring using tools as the one presented in this work could have valuable significance to decision-makers, industry and Governments.

In ocean colour remote sensing applications, the atmospheric correction model has to be performed accurately since any error from the atmospheric correction stage will affect the estimation of the biophysical parameters. S2 and L8 were mainly designed for terrestrial vegetation applications, so a precise atmospheric correction scheme is required for the development of water quality algorithms. In this study, ACOLITE DSF algorithm performed accurately over the study area for both S2 and L8 satellites, and minimal sun glint effects are visible in the images, as provided with similar reflectance values for pixels inside and outside the algal bloom compared to those of S3 (Fig. 9). This algorithm has been already validated in several areas with optical complex waters (Caballero et al., 2018, 2019; Renosh et al., 2020), as in other studies about flagellates as *Lingulodinium polyedra* by Caballero et al. (2020). Landsat satellites do not have bands in the red-edge spectral range (700–720 nm). This feature distinguishes the optical signature of the Sentinels compared to that of L8, which loses the capacity of the potential application of new algorithms for some precise marine
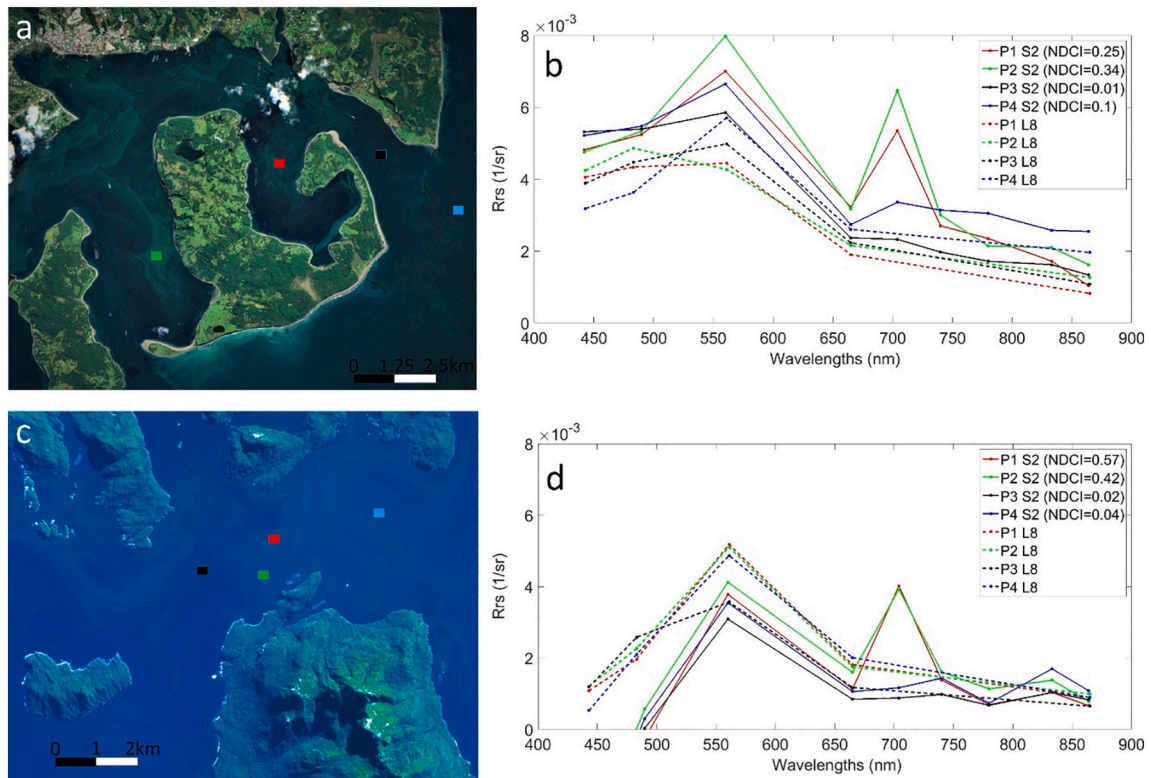
**Fig. 10.** a, c) RGB (red-green-blue) composites from S2 in the two study areas of Cailin Island (South of Chiloe Island) and Melimoyu bay, respectively, b, d) Comparison of the reflectance spectra from S2 and L8 in some pixels (P1, P2, P3, and P4) for each respective area. The normalized difference chlorophyll index (NDCI) values are indicated for each S2 pixel. (For interpretation of the references to colour in this figure legend, the reader is referred to the web version of this article.)

applications. Currently, both S2A and S2B are in orbit, providing a five-day revisit frequency at the equator and better temporal resolution at higher latitudes. This will allow monitoring for algal blooms, even in small geographic areas where the 300 m spatial resolution of S3 is not sufficient. However, one of the key handicaps for the implementation of an operational remote sensing system is the cloud influence, especially in the higher latitudes of the Patagonian inner water systems. As previously mentioned, cloud coverage data based on the annual observations from Puerto Montt meteorological station (Code 410005; 41.447° S; 73.095° W) indicated from last 2019 annual report that 49% of days had severe cloud coverage. Nevertheless, taking into account that during summer and early autumn, when lower cloud coverage is encountered and mainly major HAB events occur in the region, remote sensing can be a valid tool within any NRT operational system. In addition, a multi-sensor approach using both S2 and S3 is also preferable for the operational and complete monitoring of algal bloom detection over broader regions. These new capabilities offer coastal water managers novel powerful tools for assessing the condition of their water bodies more frequently and synoptically, which will allow them to focus their limited resources on mitigating the risks of potentially harmful blooms at regional to national scales.

The advantage of using next-generation optical sensors to supplement the information gathered from in situ observations of algal bloom dynamics is of key importance. Considering that the S3 and S2 missions will provide images over the coming decades, this approach could be applied for the effective routine monitoring of algal blooms along this coast. Further research should be focused on gathering field data covering a higher number of algal bloom scenarios; however, the results of this study indicate the potential of S3 and S2 as a tool for assessing the spatiotemporal dynamics of algal blooms through holistic analysis and for encouraging improved coastal management practices in the Southern coast of Chile. Traditional in situ monitoring is a rather time-

and money-consuming method for estimating HABs on a regular basis; however, they are necessary for identifying algae blooms at the species level. The relevance and added value of cal/val exercises using contemporaneous in situ HAB abundance data in tandem with satellite remote sensing is key for detecting whether a bloom is harmful or produces toxins. The application of NDCI avoids the confounding influence of CDOM and total suspended sediments, which are highly variable and significant in the southern Chilean fjords and channels. In this context, future sampling programmes will be adjusted to include measurements relevant to satellite validation, such as bio-optical properties of the water column and spectral reflectance. These new on-site data streams should be extremely useful in evaluating the performance of new HABs algorithms and will be especially relevant for a future operational satellite detection system.

Considering that Chile is a country also exposed to natural disasters (Camus et al., 2016; CFE-DMHA, 2017), remote sensing methodologies could be potentially used also in future situations. The current scenario due to COVID-19 pandemic period, which was the reason of in situ data slowdown, could happen again due to other natural or anthropogenic reasons. Therefore, satellite technology, as those available from Copernicus instruments, could be invaluable resources for decision-makers and therefore for the regional and national economy. Currently, there are platforms for aquaculture already available in Southern Chile that can integrate the new knowledge and tools generated in this study, including the PROMOFI-INTESAL (http://mapas.intesal.cl/publico/) and the SIMA Austral, SERNAPESCA (Steven et al., 2019). NRT satellite-retrieved datasets (S2, S3) might offer significant information for enhanced ecosystem management and HAB mitigation in order to routinely monitor the distribution of algal blooms within the early-alarm systems. A more holistic and multidisciplinary approach is necessary for optimal risk assessment and can improve our predictive capacity by gathering information from, at a minimum, HAB and
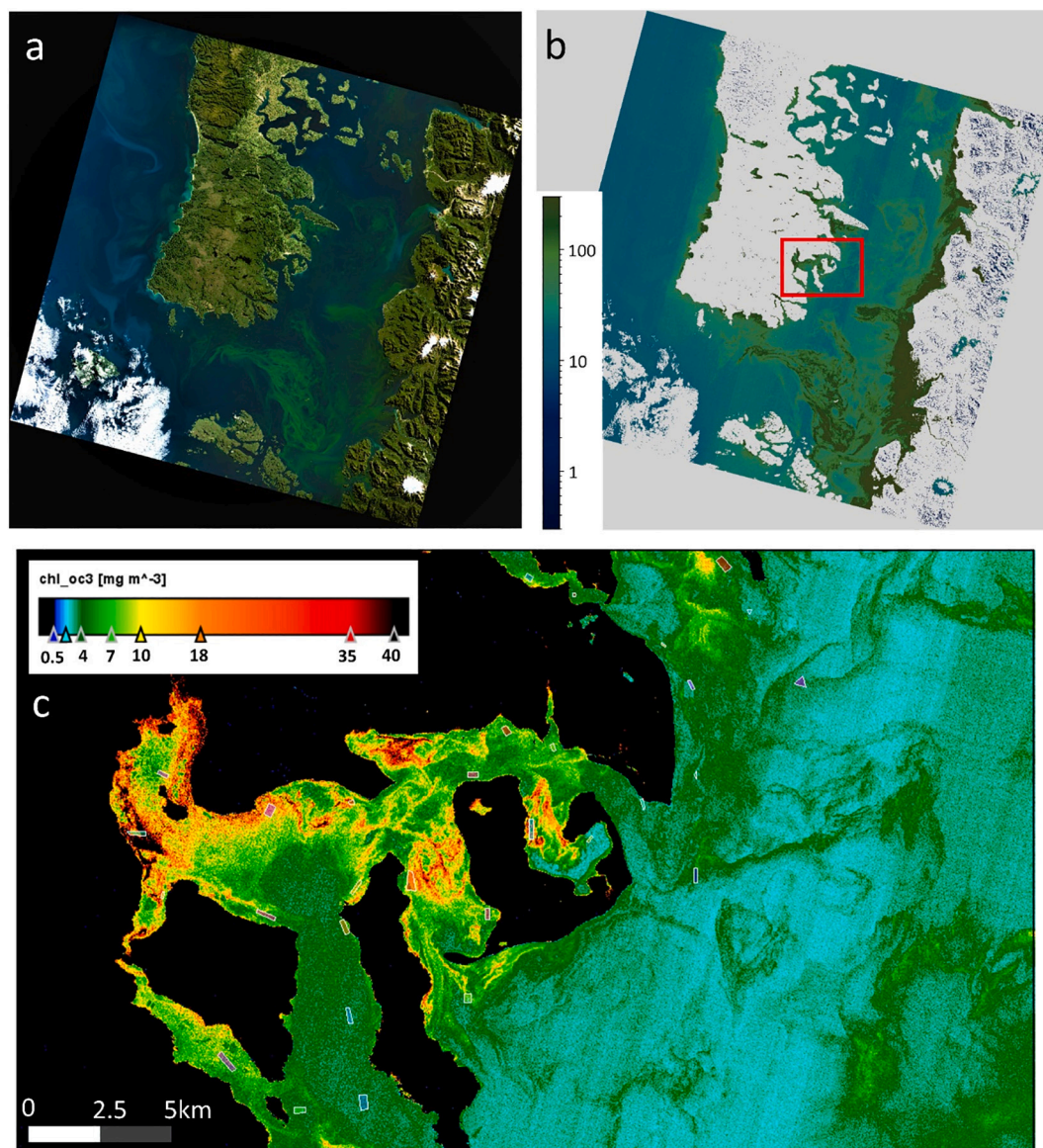
**Fig. 11.** a) RGB (red-green-blue) composite from a L8 scene acquired on 30 March 2020 at 30 m spatial resolution, b) chlorophyll map using the OC3 algorithm, and c) zoom of this map in one of the aquaculture sites recording fish mortality in the Quellón region (sector 12A). (For interpretation of the references to colour in this figure legend, the reader is referred to the web version of this article.)

biotoxin monitoring data, remote sensors and trajectory modeling. This approach is the starting point for initiatives such as the "Applied si-mulations and integrated modeling for the understanding of toxic and harmful algal blooms" (ASIMUTH) and "Predicting risk and impact of harmful events on the aquaculture sector" (PRIMROSE) projects (Maguire et al., 2016). In addition, using satellites to detect HABs can foster faster decision-making that reduces harm to public health as well as associated costs. In a new study, Stroming et al. (2020) described a framework for quantifying socioeconomic benefits of monitoring HABs with satellites. By looking at a series of case studies, the researchers consider how decision-makers might change approaches when satellite data are available and whether the data lead to decisions that reduce harm and save money. Our study suggests that both S3 and S2 Co-pernicus operational data can detect HABs in NRT for an improved management of fisheries and aquaculture advisories in Chile. Co-pernicus makes available a large amount of optical and microwave data obtained from satellites, not only in an operational way, but also through long time-series of data obtained since the beginning of each Earth Observation mission. Therefore, this information can be the

baseline of many future applied science studies in benefit of the knowledge and protection of the environment, the understanding of natural or anthropogenic phenomena as harmful phytoplankton blooms and for the reinforcement of the sustainability of the socioeconomic activities.

## 5. Conclusions

The operational availability of data from the Copernicus programme allowed us to monitor, in near real time, oceanographic events with a high socio-economic impact, such as the harmful phytoplankton bloom occurred in southern Chile, which was confirmed by the authorities with in situ data. Local samplings from the regional monitoring pro-gramme were slowed down during the COVID-19 lockdown due to the confinement. However, satellite imagery allowed daily observation of the algal bloom at the end of the austral summer 2020 and, therefore, advises to decision-makers on time to be prepared for possible massive salmon mortalities events on the aquaculture sites. Harmful algal blooms containing the dinoflagellates *Cochlodinium polykrikoides* and

*Lepidodinium chlorophorum* were monitored at mesoscale and local scales, with accurate spatial and temporal observations in areas where fish farmers reported salmon mortalities. The harmful species had a strong reflectance response in the near infrared part of the spectra, which allowed the detection of this peak using the adequate spectral bands of Sentinel-2 and Sentinel-3 satellites. This advantage can be exploited using the reflectance-based algorithm normalized difference chlorophyll index (NDCI) as a powerful tool. Copernicus data was used in this area for the first time in an operational way and allowed monitoring aspects of the marine environment independently from the terrestrial or maritime logistics. This provides a key benefit to increase technical value added information for decision-makers in situations of natural catastrophes and blockages, such as those that occurred during the global COVID-19 lockdown.

## CRediT authorship contribution statement

All authors contributed equally to this paper. Isabel Caballero supervised and coordinated the research.

## Declaration of competing interest

The authors declare that they have no known competing financial interests or personal relationships that could have appeared to influence the work reported in this paper.

## Acknowledgements

## References

Anderson, D.M., 1995. ECOHAB: The Ecology and Oceanography of Harmful Algal Blooms: A National Research Agenda. Woods Hole Oceanographic Institution, Woods Hole, MA (66 pp).

Anderson, D.M., Rensel, J., 2016. Harmful algal blooms. Assessing Chile's historic HAB events of 2016. https://www.aquaculturealliance.org/wp-content/uploads/2017/05/Final-Chile-report.pdf.

Anderson, D.M., Cembella, A.D., Hallegraeff, G.M., 2012. Progress in understanding harmful algal blooms: paradigm shifts and new technologies for research, monitoring, and management. Annu. Rev. Mar. Sci. 4, 143–176.

Aqua Report, 2020a. https://www.aqua.cl/2020/04/14/sernapesca-activa-plan-de-contingencia-ante-mortalidad-masiva-en-centro-de-marine-farm/ (14 April).

Aqua Report, 2020b. https://www.aqua.cl/2020/04/07/sernapesca-verifica-retiro-de-la-mortalidad-masiva-desde-centro-afectado-por-microalga/ (7 April).

Armijo, J., Oerder, V., Auger, P.A., Bravo, A., Molina, E., 2020. The 2016 red tide crisis in southern Chile: possible influence of the mass oceanic dumping of dead salmons. Mar. Pollut. Bull. 150, 110603.

Caballero, I., Steinmetz, F., Navarro, G., 2018. Evaluation of the first year of operational Sentinel-2A data for retrieval of suspended solids in medium-to high-turbidity waters. Remote Sens. 10 (7), 982.

Caballero, I., Ruiz, J., Navarro, G., 2019. Sentinel-2 satellites provide near-real time evaluation of catastrophic floods in the west Mediterranean. Water 11 (12), 2499.

Caballero, I., Fernández, R., Escalante, O.M., Mamán, L., Navarro, G., 2020. New capabilities of Sentinel-2A/B satellites combined with in situ data for monitoring small harmful algal blooms in complex coastal waters. Sci. Rep. 10 (1), 1–14.

Cáceres, M., Valle-Levinson, A., Sepúlveda, H.H., Holderied, K., 2002. Transverse variability of flow and density in a Chilean fjord. Cont. Shelf Res. 22 (11−13), 1683–1698.

Cáceres, M., Valle-Levinson, A., Atkinson, L., 2003. Observations of cross-channel structure of flow in an energetic tidal channel. J. Geophys. Res. Oceans 108 (C4).

Camus, P., Arenas, F., Lagos, M., Romero, A., 2016. Visión histórica de la respuesta a las amenazas naturales en Chile y oportunidades de gestión del riesgo de desastre. Revista de Geografía Norte Grande (64), 9–20.

Castillo, M., Velenzuela, C., 2008. Circulation regime in the austral Chilean channels and fjords. In: Silva, N., Palma, S. (Eds.), Progress in the Oceanographic Knowledge of Chilean Interior Waters, From Puerto Montt to Cape Horn. Comité Oceanográfico Nacional-Pontificia Universidad Católica de Valparaíso, Valparaíso, Chile, pp. 59–62.

Center for Excellence in Disaster Management & Humanitarian Assistance, CFE-DMHA, 2017. Chile: Disaster Management Reference Handbook, May 2017. https://reliefweb.int/report/chile/chile-disaster-management-reference-handbook-may-2017.

Cerda, E., 2019. Productividad y competitividad en la industria del salmón en Chile. Cieplan. 109 pp. http://www.cieplan.org/wp-content/uploads/2019/09/PAPER-EDGARDO-CERDA-bajares.pdf Editorial: Javiera Pérez M. ISBN: 978-956-204-086-0.

Clement, A., Lincoqueo, L., Saldivia, M., Brito, C.G., Muñoz, F., Fernández, C., ... Contreras, G., 2016. Exceptional summer conditions and HABs of *Pseudochattonella* in Southern Chile create record impacts on salmon farms. Harmful Algae News 53, 1–3.

Cortes, D.L., Nuñez Vazquez, E., Dorantes-Aranda, J., Band-Schmidt, C., Sandoval, F.H., Bustillos-Guzman, J., Leyva Valencia, I., 2019. The state of knowledge of harmful algal blooms of *Margalefidinium* (*Cochlodinium*) *polykrikoides* in Latin America. Front. Mar. Sci. 6, 463.

Cullen, J.J., 2008. Observation and Prediction of Harmful Algal Blooms. Real-time Coastal Observing System for Marine Ecosystem Dynamics and Harmful Algal Blooms: Theory, Instrument and Modeling. UNESCO, Paris.

Díaz, P.A., Álvarez, A., Varela, D., Pérez-Santos, I., Díaz, M., Molinet, C., ... Rengel, J., 2019. Impacts of harmful algal blooms on the aquaculture industry: Chile as a case study. Perspect. Phycol. 6 (1–2), 39–50.

Dwivedi, R., Rafeeq, M., Smitha, B.R., Padmakumar, K.B., Thomas, L.C., Sanjeevan, V.N., ... Raman, M., 2015. Species identification of mixed algal bloom in the Northern Arabian Sea using remote sensing techniques. Environ. Monit. Assess. 187 (2), 51.

European Organization for the Exploitation of Meteorological Satellites – EUMETSAT, 2018. Sentinel-3 OLCI Marine User Handbook. pp. 1–41.

European Space Agency – ESA, 2019. Sentinel-3 OLCI Technical Guide. https://sentinel.esa.int/web/sentinel/user-guides/sentinel-3-olci.

European Space Agency – fESA, 2015. Sentinel-2 User Handbook. ESA Standard Document. European Space Agency, Paris, France.

Glibert, P.M., Burkholder, J.M., 2006. The complex relationships between increases in fertilization of the earth, coastal eutrophication and proliferation of harmful algal blooms. In: Ecology of Harmful Algae. Springer, Berlin, Heidelberg, pp. 341–354.

Glibert, P.M., Icarus Allen, J., Artioli, Y., Beusen, A., Bouwman, L., Harle, J., ... Holt, J., 2014. Vulnerability of coastal ecosystems to changes in harmful algal bloom distribution in response to climate change: projections based on model analysis. Glob. Chang. Biol. 20 (12), 3845–3858.

Gobler, C.J., 2020. Climate change and harmful algal blooms: insights and perspective. Harmful Algae 91, 101731.

Gómez, F., Richlen, M.L., Anderson, D.M., 2017. Molecular characterization and morphology of *Cochlodinium strangulatum*, the type species of *Cochlodinium*, and *Margalefidinium* gen. nov. for *C. polykrikoides* and allied species (*Gymnodiniales, Dinophyceae*). Harmful Algae 63, 32–44.

Gower, J., 2016. On the use of satellite-measured chlorophyll fluorescence for monitoring coastal waters. Int. J. Remote Sens. 37 (9), 2077–2086.

Gower, J., King, S., Borstad, G., Brown, L., 2005. Detection of intense plankton blooms using the 709 nm band of the MERIS imaging spectrometer. Int. J. Remote Sens. 26 (9), 2005–2012.

Gower, J., King, S., Goncalves, P., 2008. Global monitoring of plankton blooms using MERIS MCI. Int. J. Remote Sens. 29 (21), 6209–6216.

Griffith, A.W., Doherty, O.M., Gobler, C.J., 2019. Ocean warming along temperate western boundaries of the Northern Hemisphere promotes an expansion of *Cochlodinium polykrikoides* blooms. Proc. R. Soc. B 286 (1904), 20190340.

Han, B., Zhu, J., Li, T., Li, J., Jia, D., Guo, K., Zhifeng, L., 2019. Preliminary validation of Sentinel-3A OLCI bio-optical products in South China Sea. In: IGARSS 2019 IEEE International Geoscience and Remote Sensing Symposium, pp. 7877–7880.

He, X., Chen, J., Wu, D., Wang, J., Xin, M., Liu, L., ... Wang, B., 2020. Occurrence, distribution, source, and influencing factors of lipophilic marine algal toxins in Laizhou Bay, Bohai Sea, China. Mar. Pollut. Bull. 150, 110789.

Hunter, P.D., Tyler, A.N., Carvalho, L., Codd, G.A., Maberly, S.C., 2010. Hyperspectral remote sensing of cyanobacterial pigments as indicators for cell populations and toxins in eutrophic lakes. Remote Sens. Environ. 114 (11), 2705–2718.

Jegou, K., 2013. Identification satellitaire des efflorescences de deux dinoflagellés, *Lepidodinium chlorophorum* et *Karenia mikimotoi*, grâce à leurs caractéristiques optiques. http://archimer.ifremer.fr/doc/00158/26912/.

Judice, T.J., Widder, E.A., Falls, W.H., Avouris, D.M., Cristiano, D.J., Ortiz, J.D., 2020. Field-validated detection of *Aureoumbra lagunensis* brown tide blooms in the Indian River Lagoon, Florida using Sentinel-3A OLCI and ground-based hyperspectral spectroradiometers. GeoHealth 4 (6), e2019GH000238.

Kim, Y., Yoo, S., Son, Y.B., 2016. Optical discrimination of harmful *Cochlodinium polykrikoides* blooms in Korean coastal waters. Opt. Express 24 (22), A1471–A1488.

Klemas, V., 2012. Remote sensing of algal blooms: an overview with case studies. J. Coast. Res. 28 (1A), 34–43.

Knight, E.J., Kvaran, G., 2014. Landsat-8 operational land imager design, characterization and performance. Remote Sens. 6 (11), 10286–10305.

Kwiatkowska, E., 2018. EUMETSAT ocean colour services. In: IOCCG'23 Committee Meeting, 6–9 March 2018.

Lara, C., Saldías, G.S., Westberry, T.K., Behrenfeld, M.J., Broitman, B.R., 2017. First assessment of MODIS satellite ocean color products (OC3 and nFLH) in the Inner Sea of Chiloé, northern Patagonia. Lat. Am. J. Aquat. Res. 45 (4), 822–827.

Lembeye, G., 2008. 6.3. Harmful algal blooms in the austral Chilean channels and fjords.

In: Silva, Palma (Eds.), Progress in the Oceanographic Knowledge of Chilean Interior Waters, From Puerto Montt to Cape Horn. CONA-P, Valparaíso, Chile, pp. 99–103.

León-Muñoz, J., Urbina, M.A., Garreaud, R., Iriarte, J.L., 2018. Hydroclimatic conditions trigger record harmful algal bloom in western Patagonia (summer 2016). Sci. Rep. 8 (1), 1–10.

Luxoro, C., 2018. Historia del Huirihue en Chile. Florecimientos Algales Nocivos. Fundación Terram 68.

Maguire, J., Cusack, C., Ruiz-Villarreal, M., Silke, J., McElligott, D., Davidson, K., 2016. Applied simulations and integrated modelling for the understanding of toxic and harmful algal blooms (ASIMUTH): integrated HAB forecast systems for Europe's Atlantic Arc. Harmful Algae 53, 160–166.

Mardones, J.I., Clement, A., 2016. Manual de Microalgas del Sur de Chile. (186 pp. ISBN 978-956-362-711-4).

Mascareño, A., Cordero, R., Azócar, G., Billi, M., Henríquez, P.A., Ruz, G.A., 2018. Controversies in social-ecological systems. Ecol. Soc. 23 (4).

Mishra, S., Mishra, D.R., 2012. Normalized difference chlorophyll index: a novel model for remote estimation of chlorophyll-a concentration in turbid productive waters. Remote Sens. Environ. 117, 394–406.

Molkov, A.A., Fedorov, S.V., Pelevin, V.V., Korchemkina, E.N., 2019. Regional models for high-resolution retrieval of chlorophyll a and TSM concentrations in the Gorky Reservoir by Sentinel-2 imagery. Remote Sens. 11 (10), 1215.

Morozov, E., Pozdnyakov, D., Smyth, T., Sychev, V., Grassl, H., 2013. Space-borne study of seasonal, multi-year, and decadal phytoplankton dynamics in the Bay of Biscay. Int. J. Remote Sens. 34 (4), 1297–1331.

Moutzouris-Sidiris, I., Topouzelis, K., Konstantinidou, E.E., 2019. Assessment of chlorophyll-a concentration derived from Sentinel-3 satellite images using open source data. In: Seventh International Conference on Remote Sensing and Geoinformation of the Environment. vol. 11174. International Society for Optics and Photonics, pp. 1117413.

Mueller, J.L., 1979. Prospects for measuring phytoplankton bloom extent and patchiness using remotely sensed ocean color images: an example. In: Toxic Dinoflagellate Blooms. Elsevier, North Holland, Inc., New York, pp. 303–308.

Mundo acuícola, 14 April 2020. https://www.mundoacuicola.cl/new/noticias/salmonicultura/activan-plan-de-contingencia-ante-mortalidad-masiva-de-salmones-en-centro-de-la-region-de-aysen/3.

Noh, J.H., Kim, W., Son, S.H., Ahn, J.H., Park, Y.J., 2018. Remote quantification of *Cochlodinium polykrikoides* blooms occurring in the East Sea using geostationary ocean color imager (GOCI). Harmful Algae 73, 129–137.

Ogashawara, I., 2019. The use of Sentinel-3 Imagery to monitor cyanobacterial blooms. Environments 6 (6), 60.

Onitsuka, G., Miyahara, K., Hirose, N., Watanabe, S., Semura, H., Hori, R., ... Yamaguchi, M., 2010. Large-scale transport of *Cochlodinium polykrikoides* blooms by the Tsushima Warm Current in the southwest Sea of Japan. Harmful Algae 9 (4), 390–397.

Palenzuela, J.M.T., Vilas, L.G., Aláez, F.M.B., Pazos, Y., 2019. Potential application of the new sentinel satellites for monitoring of harmful algal blooms in the Galician aquaculture. Thalassas 1–9.

Parsons, T.R., Maita, Y., Lally, C.M., 1985. Pigments. A Manual of Chemical and Biological Methods for Seawater Analysis. Pergamon Press, Oxford, pp. 101–104.

Pitcher, G., Jacinto, G.S., 2019. Ocean deoxygenation links to harmful algal blooms. In: Ocean Deoxygenation: Everyone's Problem-Causes, Impacts, Consequences and Solutions. Publisher: IUCN, Gland, Switzerland.

Renosh, P.R., Doxaran, D., Keukelaere, L.D., Gossn, J.I., 2020. Evaluation of atmospheric correction algorithms for Sentinel-2-MSI and Sentinel-3-OLCI in highly turbid estuarine waters. Remote Sens. 12 (8), 1285.

Rodríguez-Benito, C., 2019. Experiencias de 16 años aportando al conocimiento de Chile mediante tecnología satelital. Seminarios Copernicus Chile. http://copernicus-chile.cl/eventos/.

Rodríguez-Benito, C., Haag, C., 2004. Applications of ENVISAT data in the south of Chile. Monitoring algal blooms and other coastal ocean features using MERIS and AATSR imagery. Gayana 68 (2), 508–513.

Rodriguez-Benito, C.V., Haag, C., 2016. Remote Sensing of Recent Huge Algal Blooms With High Socio-economic Impact in the Southern Pacific Coast. Color and Light in the Ocean from EO (CLEO), Frascati (Italy), 6–8 Sept. 2016.

Rodríguez-Benito, C., Haag, C., Fea, M., Gutiérrez, H., 2006. Monitoring marine life from space-Envisat experience in Chile. ESA Bull. 126, 42–47.

Roselli, L., Vadrucci, M.R., Belmonte, M., Ciciriello, P., Rubino, F., Ungaro, N., Caroppo, C., 2020. Two-stages bloom of *Margalefidinium cf. polykrikoides* in a Mediterranean shallow bay (Ionian Sea, Italy). Mar. Pollut. Bull. 151, 110825.

Sakuno, Y., Maeda, A., Mori, A., Ono, S., Ito, A., 2019. A simple red tide monitoring method using Sentinel-2 data for sustainable management of Brackish Lake Koyama-ike, Japan. Water 11 (5), 1044.

Sandoval, M., Parada, C., Torres, R., 2018. Proposal of an integrated system for forecasting Harmful Algal Blooms (HAB) in Chile. Lat. Am. J. Aquat. Res. 46 (2), 424–451.

Sernapesca, 2017. Manual de implementación de la normativa excepcional aplicable ante eventos de mortalidades masivas. February 2017. 21 pp. http://www.sernapesca.cl/manuales-publicaciones/obligaciones-ante-mortalidades-masivas-en-centros-de-salmonidos.

Sernapesca, 2020. Report 5/2020. Boletín Estado de Floraciones de Algas Nocivas (FAN). Programa de vigilancia, detección y control de monitoreo fitoplancton nocivo (Res. Ex. N° 2198/2017). Departamento de Gestión Ambiental.

Smith, M.E., Bernard, S., 2020. Satellite ocean color based harmful algal bloom indicators for aquaculture decision support in the Southern Benguela. Front. Mar. Sci. 7, 61.

Son, Y.B., Ishizaka, J., Jeong, J.C., Kim, H.C., Lee, T., 2011. *Cochlodinium polykrikoides* red tide detection in the South Sea of Korea using spectral classification of MODIS data. Ocean Sci. J. 46 (4), 239–263.

Sourisseau, M., Jegou, K., Lunven, M., Quere, J., Gohin, F., Bryere, P., 2016. Distribution and dynamics of two species of *Dinophyceae* producing high biomass blooms over the French Atlantic Shelf. Harmful Algae 53, 53–63.

Steven, A.D., Aryal, S., Bernal, P., Bravo, F., Bustamante, R.H., Condie, S., ... Herzfeld, M., 2019. SIMA Austral: an operational information system for managing the Chilean aquaculture industry with international application. J. Oper. Oceanogr. 12 (sup2), S29–S46.

Stroming, S., Robertson, M., Mabee, B., Kuwayama, Y., Schaeffer, B., 2020. Quantifying the human health benefits of using satellite information to detect cyanobacterial harmful algal blooms and manage recreational advisories in US Lakes. GeoHealth 4 (9), e2020GH000254.

Subpesca, 2019. Informe Sectorial de Pesca y Acuicultura 2019. http://www.subpesca.cl/portal/616/articles-106845_documento.pdf.

Toming, K., Kutser, T., Laas, A., Sepp, M., Paavel, B., Nõges, T., 2016. First experiences in mapping lake water quality parameters with Sentinel-2 MSI imagery. Remote Sens. 8 (8), 640.

Vanhellemont, Q., 2019. Adaptation of the dark spectrum fitting atmospheric correction for aquatic applications of the Landsat and Sentinel-2 archives. Remote Sens. Environ. 225, 175–192.

Vanhellemont, Q., Ruddick, K., 2016. Acolite for Sentinel-2: aquatic applications of MSI imagery. In: Proceedings of the 2016 ESA Living Planet Symposium, Prague, Czech Republic, pp. 9–13.

Vanhellemont, Q., Ruddick, K., 2018. Atmospheric correction of metre-scale optical satellite data for inland and coastal water applications. Remote Sens. Environ. 216, 586–597.

Villanueva, F., Urrutia, G., Uribe, C., Seguel, M., Aguilera-Belmonte, A., Olivares, B., ... Paredes, J., 2016. Harmful Algal Bloom of *Pseudochattonella verruculosa (Dictyochophyceae, Florenciellales)* associated with salmon farm mortalities in the South of Chile. In: Conference ICHA.

Woodcock, C.E., Allen, R., Anderson, M., Belward, A., Bindschadler, R., Cohen, W., ... Nemani, R., 2008. Free access to Landsat imagery. Science 320, 1011.

Yunus, A.P., Masago, Y., Hijioka, Y., 2020. COVID-19 and surface water quality: improved lake water quality during the lockdown. Sci. Total Environ. 731, 139012.

Zambrano-Monserrate, M.A., Ruano, M.A., Sanchez-Alcalde, L., 2020. Indirect effects of COVID-19 on the environment. Sci. Total Environ. 138813.

Zhang, Y., Chen, C., Xue, P., Beardsley, R.C., Franks, P.J., 2020. A view of physical mechanisms for transporting harmful algal blooms to Massachusetts Bay. Mar. Pollut. Bull. 154, 111048.